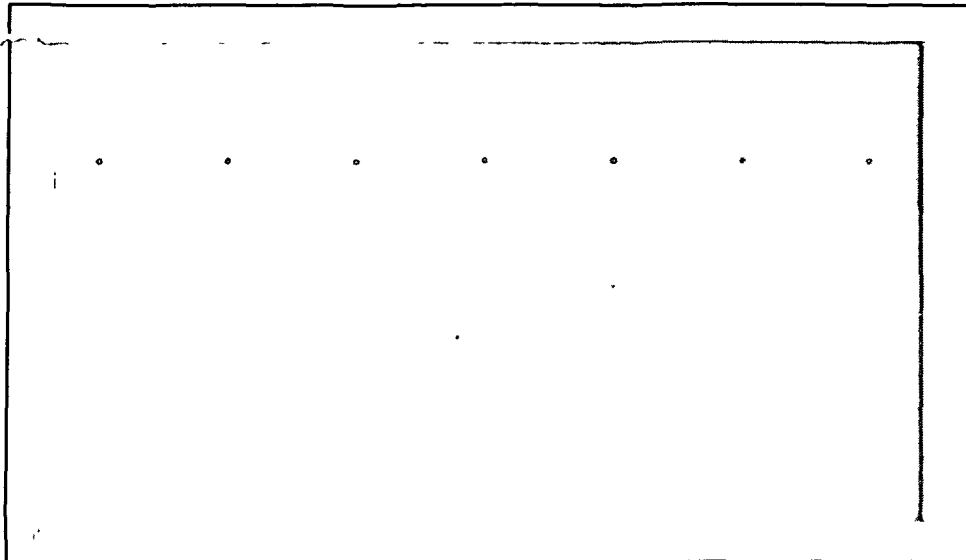


NA 8 3-382



Drexel
University



College of Engineering
Department of
Mechanical Engineering
and Mechanics
Philadelphia, PA 19104

(215) 895-2352-53



(NASA-CR- 176564) COMBUSTION CHARACTERISTICS
IN THE TRANSITION REGION OF LIQUID FUEL
SPRAYS Final Report, Jan. 1983 - Sep. 1985
(Drexel Univ.) 56 p HC A04/MF A01 CSCL 21B

N86-20517

Unclassified
G3/25 05582

**COMBUSTION CHARACTERISTICS IN THE
TRANSITION REGION OF LIQUID FUEL SPRAYS**

Final Report

January 1983 - September 1985

N. P. Cernansky, I. Namer and R. J. Tidona

January 1986

**Research Supported by the NASA-Lewis Research Center
NASA Research Grant Award **NAG 3-382****

**Opinions, findings, and conclusions or recommendations
are those of the authors and do not necessarily reflect the views of NASA**

**MECHANICAL ENGINEERING AND MECHANICS DEPARTMENT
DREXEL UNIVERSITY
PHILADELPHIA, PA 19104**

ABSTRACT

A number of important effects have been observed in the droplet size transition region in spray combustion systems. In this region, where the mechanism of flame propagation is transformed from diffusive to premixed dominated combustion, the following effects have been observed: (1) maxima in burning velocity; (2) extension of flammability limits, (3) minima in ignition energy; and (4) minima in NO_x formation. Unfortunately, because of differences in experimental facilities and limitations in the ranges of experimental data, a unified description of these transition region effects is not available at this time. Consequently, a fundamental experimental investigation was initiated in January 1983 to study the effect of droplet size, size distribution, and operating parameters on these transition phenomena in a single well controlled spray combustion facility.

A monodisperse aerosol generator has been used to form and deliver a well controlled liquid fuel spray to the combustion test section where measurements of ignition energy have been made. The ignition studies were performed on monodisperse n-heptane sprays at atmospheric pressure over a range of equivalence ratios and droplet diameters. A capacitive discharge spark ignition system was used as the ignition source, providing independent control of spark energy and duration.

Preliminary measurements were made to optimize spark duration and spark gap, optimum conditions being those at which the maximum frequency or probability of ignition was observed. Using the optimum electrode spacing and spark duration, the frequency of ignition was determined as a function of spark energy for three overall equivalence ratios (0.6, 0.8, and 1.0) and for initial droplet diameters of 25, 40, 50, 60, and 70 μm . An LDA system was used to

determine the actual equivalence ratio at the spark gap, which varied from 1.5 to 4.7. The spark energy at which the frequency of ignition was 90 percent was defined as the minimum ignition energy.

These data indicated that the ignitability of the sprays was enhanced as the equivalence ratio was increased, but was diminished as the droplet size was increased. The increase in minimum ignition energy with increasing droplet size and fixed equivalence ratio was nearly linear over the range of parameters studied. However, the effect became smaller with increasing equivalence ratio.

Optical in situ particle sizing of fuel droplets has been developed to better characterize droplet size distribution, number density, and extent of prevaporation at the test section (spark gap in the case of the minimum ignition energy studies). Numerical calculations using a newly developed Mie scattering computer code have been made to provide information critical to optimizing the optics for the laser-based droplet sizing technique. This method is a single particle counter which measures near forward scattering and uses light detection at 90 degrees to the laser beam to constrain the probe volume to the central portion of the beam only. This technique can provide accurate measurement of droplet sizes in the 10-100 μm range, is relatively insensitive to particle index of refraction, and can handle realistic spray number densities.

TABLE OF CONTENTS

	Page
ABSTRACT	ii
TABLE OF CONTENTS	iv
LIST OF FIGURES AND TABLES	v
I. INTRODUCTION AND PROGRAM OVERVIEW	1
A. Introduction	1
B. Project Summary	3
C. Recommendations for Future Work	6
D. Research Personnel and Activities	7
E. Reports and Publications	7
II. EXPERIMENTAL FACILITY	9
A. Monodisperse Spray Generator	9
B. Spark Ignition Apparatus	11
C. Laser Doppler Anemometer	13
D. Droplet Size Measurement	15
III. EXPERIMENTAL RESULTS AND DISCUSSION	21
A. Effect of Spark Duration on Minimum Ignition Energy	21
B. Spark Gap Equivalence Ratio Determination	21
C. Optimization of Spark Gap Width	23
D. Droplet Size and Equivalence Ratio Effects on Minimum Ignition Energies	25
E. Droplet Sizing Method	31
F. Summary and Conclusions	42
IV REFERENCES	45
APPENDIX PUBLICATIONS AND PRESENTATIONS	47

LIST OF FIGURES AND TABLES

	Page
Figure 1 Schematic of Aerosol Generation and Ignition Test Facility	10
Figure 2. Schematic of Spark Generation Circuit	12
Figure 3. Schematic of Laser Doppler Anemometer System	14
Figure 4. Optical Arrangement for Droplet Sizing	17
Figure 5. Schematic of Signal Processing System for Laser Droplet Sizing Apparatus	19
Figure 6. Effect of Spark Duration on the Minimum Ignition Energy of N-Heptane Sprays: $D_0 = 68 \mu\text{m}$; $\theta = 1.0$; Spark Gap = 2.0 mm.....	22
Figure 7. Radial Profiles of Local Equivalence Ratio (θ') Across the Test Section for N-Heptane Sprays: $D_0 = 50 \mu\text{m}$; Spark Gap = 3.0 mm; Spark Duration = 77 μs	24
Figure 8 Effect of Spark Gap Width on the Frequency of Ignition for N-Heptane Sprays: $D_0 = 70 \mu\text{m}$; $\theta = 1.0$, Spark Duration = 76 μs ; Spark Energy = 0.8 mJ	26
Figure 9. Effect of Gap Equivalence Ratio (θ_G) and Spark Energy on the Frequency of Ignition for N-Heptane Sprays: $D_0 = 60 \mu\text{m}$; Spark Gap = 3.0 mm; Spark Duration = 77 μs	28
Figure 10. Effect of Gap Equivalence Ratio (θ_G) and Initial Droplet Diameter (D_0) on the Minimum Ignition Energy of N-Heptane Sprays	29
Figure 11. Collection Geometry	33

Figure 12. Computed Response Function Using Mie Theory, Optimized System	35
Figure 13. Computed Response Function Using Mie Theory, Non-Optimized System	36
Figure 14. The Effect of Collection Aperture (ϕ_L) on the Computed Response Function	38
Figure 15. The Effect of Collection Angle (ϕ_C) on the Computed Response Function	39
Figure 16. The Effect of the Imaginary Part of the Index of Refraction on the Computed Response Function	41
Table 1. Computational Matrix	34

I. INTRODUCTION AND PROGRAM OVERVIEW

A. Introduction

The combustion of liquid fuel sprays is expected to remain a major source of energy well into the twenty-first century. However, fuel properties and quality are currently deteriorating. It is anticipated that the fuels of the future may have properties which are significantly different from today's fuels. In order to effectively design fuel injectors, combustors, and ignitors to accommodate broadened specification and synthetic fuels, a more fundamental understanding of the combustion of liquid fuel sprays in the so called transition region has been undertaken at Drexel University.

The transition region is usually associated with droplets in the 10-100 μm diameter range. The following important effects have been observed in the transition region: (1) maxima in burning velocity; (2) extension of flammability limits; (3) minima in ignition energy requirements; and (4) minima in NO_x formation. Therefore, combustion in the transition region is an attractive design goal for practical combustors.

Previous research has shown that, in the transition region, control of the combustion process is transformed from diffusive to premixed domination. It has been suggested that this transformation in controlling mechanism is responsible for the observed transition region phenomena. More specifically, these phenomena are associated with the complex interactions between droplets in the size and number density range where the presence of neighboring droplets can significantly affect the evaporative and combustion environment of the fuel spray. Overall, the combustion behavior is affected by the relative fraction of fuel initially in a prevaporized and premixed state, the average interdroplet spacing, and the fuel properties. Although considerable research has been and is being undertaken in this area by a number of

investigators, a consolidated picture of these transition region phenomena and their mechanisms is not yet available. This is due in part to the very different aerosol generating techniques (generally poorly controlled polydisperse sprays), limited and dissimilar operating ranges (e.g., equivalence ratio), different combustion systems, etc. used by the various experimental investigators.

Adequate predictions of droplet interaction effects on spray ignition in the transition region are not available yet. It remains difficult to directly compare detailed model predictions with experimental data because there are little data from spray configurations which correspond to those that have been modeled. Furthermore, much of the experimental ignition data to date has been for polydisperse sprays where the drop sizes which may control the evaporation and interactions are not well characterized. Where monodisperse sprays have been used, there has generally been poor control of other variables. More specifically, several important ignition studies were for polydisperse sprays with droplets in the diameter range of 30 to 120 microns. Thus, it has not been possible to ascertain the droplet diameter at which the ignition energy requirement is truly minimized from the previous work. Also, previous work has not covered the entire transition range of droplet diameters and equivalence ratios. For these reasons, a complete and comprehensive picture of ignition energy variation in the transition region is not available. Thus, there is a need for comprehensive studies examining droplet size effects on minimum ignition energy in more detail, particularly where better control can be placed on the experimental variables.

B. Project Summary

A fundamental study was initiated in January 1983 with the support of NASA Grant Award NAG 3-382 to study the droplet size effects on (1) minimum ignition energy, (2) maximum burning velocity, and (3) extension of the flammability limits and to determine the optimum droplet diameters (if they exist). The use of a single spray combustion facility for all of this work insured uniformity in the interpretation of data and is expected to lead to the formulation of a comprehensive model of combustion in the transition region. This program followed the study of Cernansky and Sarv (1983) on NO_x formation in monodisperse fuel spray combustion.

NASA support was prematurely terminated because of funding constraints. Therefore, the effort was limited to the study of the droplet size effects on minimum ignition energies. The burning velocity studies and flammability limits study had to be abandoned at this time without proper support.

The experimental program as originally planned had the following specific objectives:

- (1) To map the minimum ignition energy for a monodisperse fuel spray combustion system in the transition region (10-80 μm initial droplet diameter) for various fuels of interest and for other important variables such as equivalence ratio, flow velocities, and fuel type;
- (2) To determine the optimum droplet diameter at which the ignition energy is minimized;
- (3) To study the effects of changing the evaporation environment on the minimum ignition energy;

- (4) To characterize the ignition requirements of polydisperse fuel sprays in terms of the droplet size distribution, and
- (5) To determine the effects of droplet size and size distribution on flame speed and flammability limits.

In the first year of the project, the design, purchase and construction of a new droplet ignition system and a new droplet sizing system were completed and the existing burner arrangement was modified. The flow geometry was changed to prevent flashback in the new configuration. The burner system now accommodates an ignition system which allows the control and measurement of ignition energy. Also, the initial design of the optical diagnostics for droplet size and velocity measurements was completed.

Since January 1984, work has concentrated on (1) the further development of the spray ignition facility to provide more repeatable data at low ignition energies; (2) minimum ignition energy experiments with n-heptane sprays at various equivalence ratios and with several droplet sizes; (3) the development of a detailed Mie scattering computer code to predict the performance parameters for the optical spray sizing system, and (4) the development of the spray sizing apparatus.

Because of initial difficulties in obtaining reliable and repeatable spark energies at the lower energies of interest, the minimum ignition energy experiments required more time than had originally been planned. Further, it had been expected that a pre-existing Mie scattering code could be readily adapted to the present optical diagnostic system. However difficulties in getting this code to run successfully on the Drexel VAX computer forced the development of an in-house code. This required significantly more time than originally planned. However, the extra time spent on the development of the ignition facility and the Mie scattering code has resulted in a more reliable and

repeatable spray sizing technique than could have been obtained without the extra effort. The result of these efforts is a highly reliable and repeatable facility for the study of spray ignition phenomena and a well-developed expertise in optical diagnostics for droplet sizing, thus providing a solid foundation for the completion of the remaining objectives of the program. These objectives include quantifying the effects of droplet size and burner operating variables on flammability limits and flame speeds.

Since the first year of work on the project (January 1983 through January 1984) was covered in detail by the last annual progress report (Cernansky et al., 1984), this final report will focus on the program efforts since that period. Section II contains a discussion of the development of the experimental facility including the monodisperse aerosol generator, spark ignition apparatus, laser Doppler anemometer, and droplet sizing system. Section III is a discussion of the experimental results for n-heptane sprays. Spark duration and gap width optimization procedures and equivalence ratio and droplet size variations are discussed in terms of their effects on minimum ignition energies. A discussion of the theory behind the droplet sizing techniques and of the results of some numerical calculations for optimizing the optical system design is given also. Section IV contains the summary and conclusions drawn from the present study.

C. Recommendations for Future Work

In order to build on the accomplishments of the present experimental and numerical efforts, we anticipate continuing our investigation of the following specific areas.

- (1) Minimum ignition energy studies of several different pure fuels, binary mixtures, and at least one actual distillate fuel;
- (2) Evaluation of flammability limit effects of droplet size and spray burner operating variables for the same fuels used in the minimum ignition energy experiments;
- (3) Studies of droplet size and spray burner operating variable effects on flame speeds for the above fuels;
- (4) Development of a pressurized spray burner facility with reactant preheat capability to extend the results of the atmospheric studies to conditions approaching those in real engines;
- (5) All of the above studies are to incorporate the new optical droplet size and size distribution measurement technique developed under the present program to make *in situ* measurements of actual droplet size. This will provide detailed information which will enable much more precise determination of local equivalence ratios and extent of prevaporation as well as droplet size and size distribution.

D. Research Personnel and Activities

The research project has been conducted under the supervision of Professors N. P. Cernansky and I. Namer as Co-Principal Investigators. They shared the responsibility for overall management of the program including conducting, directing, and reporting the research efforts. The primary responsibility for carrying out the details of the experimental and analytical efforts was shared by two graduate research assistants, Mr. Allen M. Danis and Mr. Daniel L. Dietrich, both Ph.D. candidates. Also contributing to the initial design and construction of the modified spray facility and the ignition apparatus were Dr. Hamid Sarv (then a Ph.D. candidate) and Mr. Shawn Smolsky (undergraduate research assistant). Mr. Robert J. Tidona (Laboratory Research Engineer) provided day-to-day guidance in the design and development of the experimental apparatus and testing program, as well as technical assistance in the collection and interpretation of data.

E. Reports and Publications

In addition to various interim progress reports and this final report, work conducted as part of this research program has resulted in the following publications and papers presented.

- (1) Danis, A. M., N. P. Cernansky and I. Namer, "Transition Region Ignition Characteristics of N-Heptane Fuel Sprays," Paper No. CSS/WSSCI 85-1-6B, presented at the 1985 Spring Technical Meeting of the Central and Western States Sections/The Combustion Institute, San Antonio, TX, 22-23 April 1985.
- (2) Dietrich, D. L., I. Namer and N. P. Cernansky, "Optimization of a Droplet Sizing Apparatus for in situ Measurements," Paper No. ESSCI 85-79, presented at the 1985 Eastern States Section/Combustion Institute Technical Meeting, Philadelphia, PA, 4-6 November 1985.

- (3) Danis, A. M., I. Namer and N. P Cernansky, "Minimum Ignition Energies of Rich N-Heptane Fuel Sprays in the Transition Region," Paper No ESSCI 85-26, presented at the 1985 Eastern States Section/Combustion Institute Technical Meeting, Philadelphia, PA, 4-6 November 1985.
- (4) Sarv, H. and N. P Cernansky, "Analysis of the Effects of Fuel Spray Characteristics on NO_x Formation," ASME Paper No 85-WA/HT-47, presented at the ASME Winter Annual Meeting, Miami Beach, FL, 17-22 November 1985.
- (5) Danis, A. M., N P Cernansky and I. Namer, "Ignition Characteristics of N-Heptane Fuel Sprays in the Transition Region," ASME Paper No 85-WA/HT-46, presented at the ASME Winter Annual Meeting, Miami Beach, FL, 17-22 November 1985

II. EXPERIMENTAL FACILITY

A. Monodisperse Spray Generator

Most practical combustors burn fuel sprays composed of droplets distributed over a wide range of diameters. However, in order to accurately determine droplet size effects on ignition energy, a spray of monosized droplets was used for the current work. The spray was produced by a Berglund-Liu Model 3050 Vibrating Orifice Monodisperse Aerosol Generator (Berglund and Liu, 1973). The spray is generated by applying a periodic disturbance to a liquid jet emerging from an orifice plate. This breaks the jet into discrete droplets with diameters within approximately 1% standard deviation of the mean diameter. Since one droplet is generated per cycle of disturbance, the droplet diameter can be calculated from the liquid flow rate (Q) and the frequency of disturbance (f), and is given by:

$$D = (6Q/\pi f)^{1/3}$$

A given size orifice is only capable of producing monodisperse droplets in a discrete range of diameters. However, this range can be extended by using several orifices of various diameters. For this work, orifices of 12.5, 15, 20, 22.5, 25, 30 and 35 μm diameter were used.

A schematic drawing of the aerosol generator and ignition test facility is given in Figure 1. This facility is described in detail by Danis *et al* (1985). The fuel flow to the aerosol generator is supplied by a high infusion syringe pump (Harvard Apparatus Model 901), and the disturbance frequency is applied by a function generator (Hewlett Packard model 3310A). After generation, the fuel droplets are kept from coagulating by a flow of dispersion air as they leave the dispersion cup. A dilution air flow is then added to the spray in the

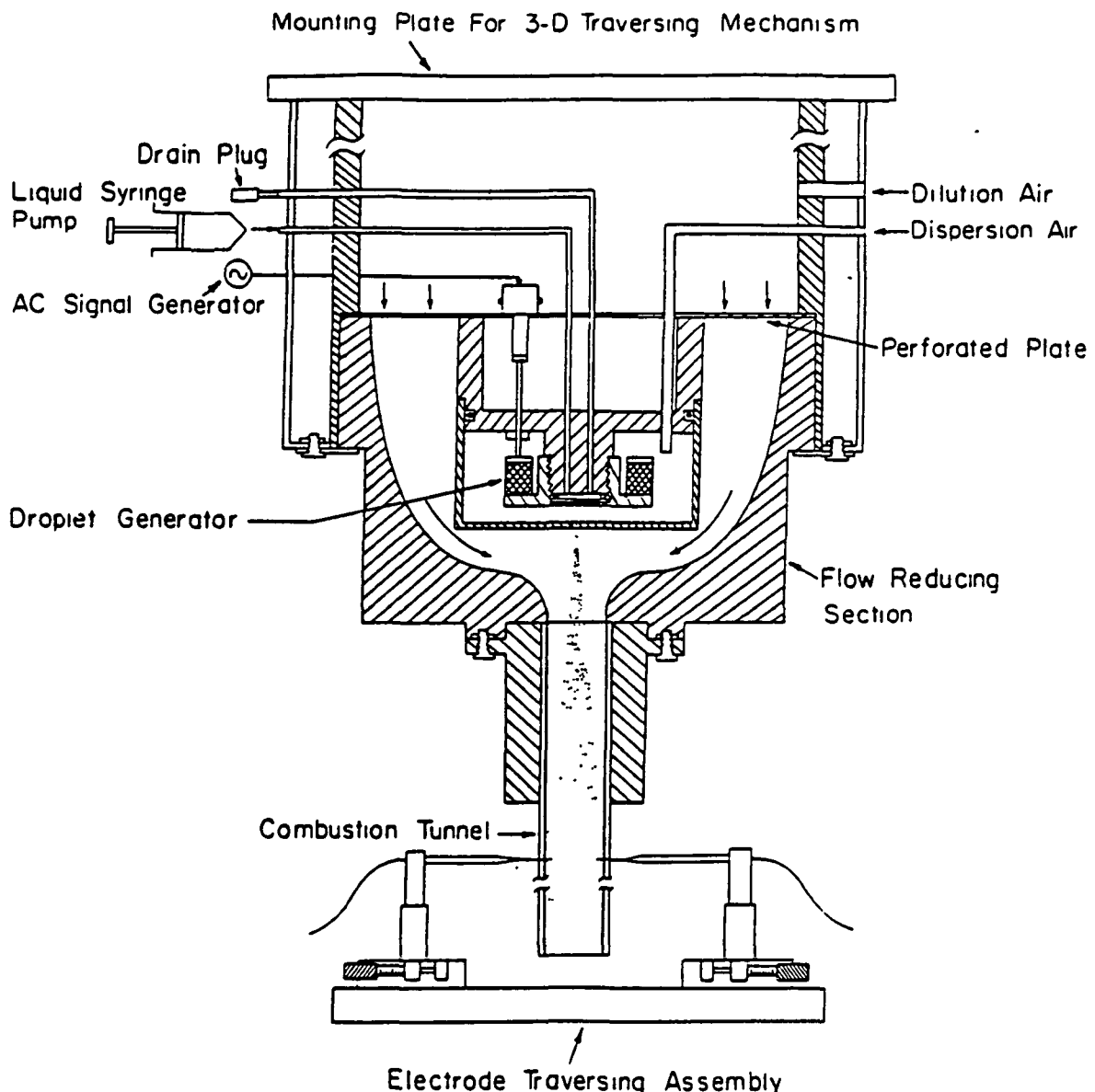


Figure 1. Schematic of Aerosol Generation and Ignition Test Facility

flow reducing section to achieve the desired overall spray stoichiometry. Both the dispersion and dilution air flows are controlled by flow controllers (Tylan Model FC-260) and monitored by mass flow meters (Hastings Model ALL-5K). The air/fuel aerosol then passes through the test section, a 13 cm i.d. pyrex tube 20 cm in length, and is vented to the atmosphere.

Electrodes are used to deliver an ignition spark to the spray in the test section at a point 8.25 cm below the orifice plate. These electrodes protrude into the test section with their main axes normal to the spray direction, and are mounted on a micrometer traversing assembly which is used to adjust the spark gap. The electrodes are 5 mm diameter stainless steel rods, with the spark-producing ends machined to 1 mm diameter and 6 mm length. The high-voltage electrode tip was pointed, while the ground-side tip was flat.

B. Spark Ignition Apparatus

A capacitive discharge spark generation system capable of independent variation of spark energy and spark duration was developed for the present study of droplet size effects on the minimum spark ignition energy of monodisperse fuel sprays. A schematic of the spark generation circuit is given in Figure 2. The spark energy and duration are independently controlled by varying the charging voltage (E_0), the capacitance (C), or the resistance (R) of the circuit. Spark energies ranging from 0.6 to 30 mJ are attainable, as well as spark durations from 5 to 150 μ s.

The spark generating procedure is as follows. The capacitor is charged to 15-25 kV by closing switch S_C . The charging resistor, R_C , limits the charging current to protect the capacitors. After charging for 3 seconds, the

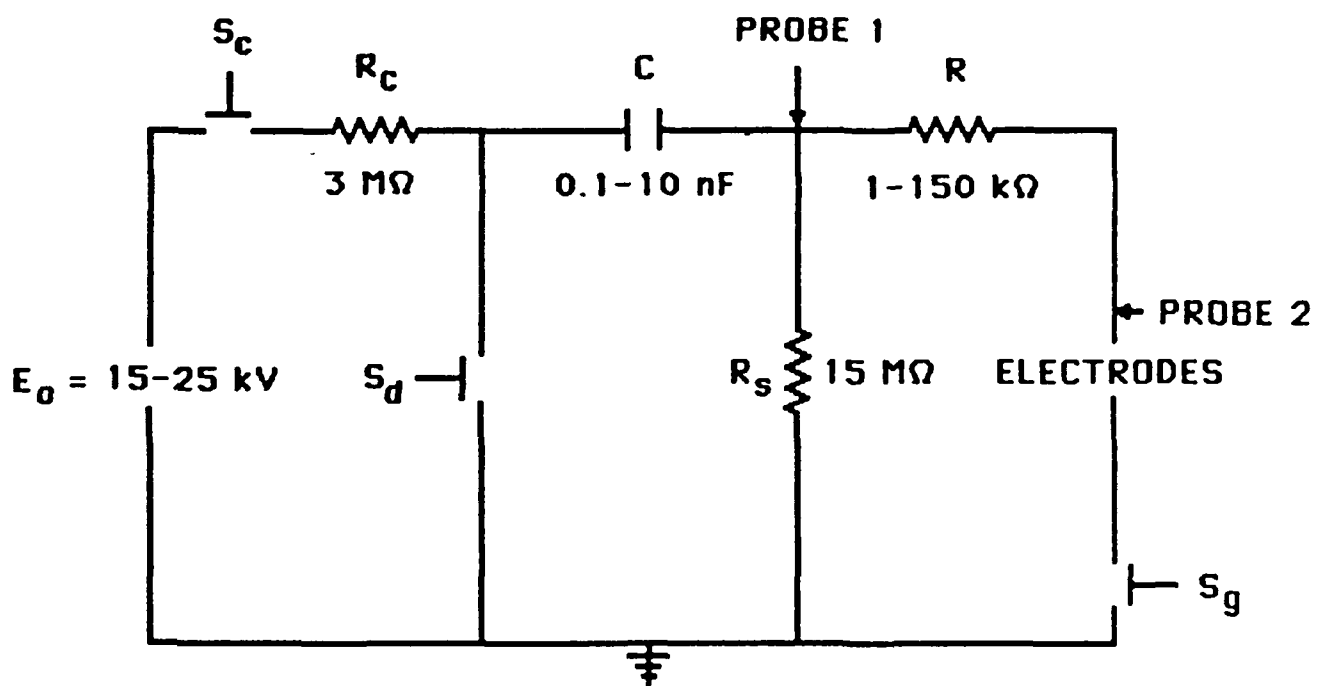


Figure 2. Schematic of Spark Generation Circuit

high voltage source is disconnected by opening S_C . The grounding switch, S_g , and the discharge switch, S_d , which are open while charging the capacitor, are then closed. This causes a large voltage difference to form across the electrodes and a spark is generated. The shunt resistor, R_s , provides an alternative path for the capacitor to discharge in the event the spark cannot jump the spark gap. S_C , S_d and S_g are high voltage solenoid switches, and the charge-discharge cycle is controlled by timing relays.

To measure the spark energy, two high voltage probes were connected to the circuit across the resistor, as seen in Figure 2, and the voltage traces of the spark were recorded on a digital oscilloscope (Norland Prowler). The voltage difference across R divided by the value of R gave the spark current, I . The spark energy, E , was determined from:

$$E = \int_0^t V(t)I(t)dt$$

where V was the measured voltage drop across the electrodes during the spark, as measured by probe 2, and t was time. The upper limit of the integration, t , was the spark duration. This was taken equal to four times the time constant of the current trace. The above integral was evaluated using the waveform processing capabilities of the digital oscilloscope.

C. Laser Doppler Anemometer

Due to the nature of the spray generation system used in this work, the droplet density, and therefore the local equivalence ratio, was not radially uniform across the test section. An approach whereby a laser Doppler anemometer (LDA) system was used to determine the actual equivalence ratio of the spray in the spark gap was developed. A detailed schematic drawing of the LDA system used is given in Figure 3.

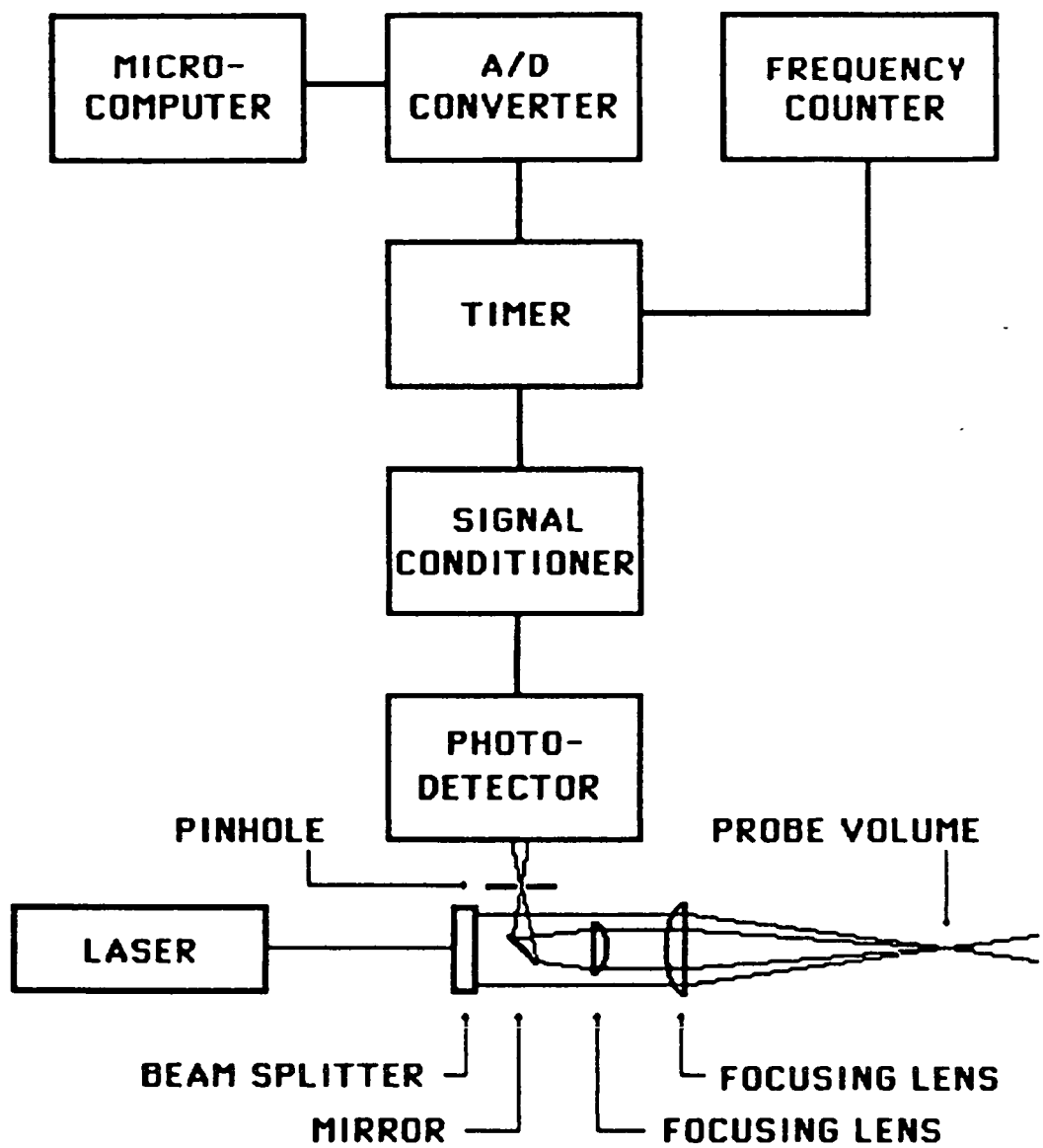


Figure 3. Schematic of Laser Doppler Anemometer System

The light source was a 35 mW Spectra Physics He-Ne Laser (Model 124B). The beam passed through a beam splitter and focusing lens to the probe volume in the spray. The backscatter mode collecting optics consisted of a collimating lens, mirror, pinhole and TSI Model 962 Photodetector. The signal was processed by a TSI Model 1984 signal conditioner and a TSI Model 1985 timer. One output of the timer led to a Monsanto Model 100B Frequency Counter for droplet rate measurements. A second output of the timer led to an A/D converter in a DEC LSI-11/2 microcomputer, which performed mean droplet velocity calculations.

The LDA was used to measure the mean droplet velocity (v) and the droplet rate (n) simultaneously at discrete radial positions across the test section. At each radial location, the ratio $n' = n/v$ was proportional to the local equivalence ratio (θ'). The average, $\langle n' \rangle$, of n' over the entire cross section was proportional to the overall equivalence ratio, θ , so the local equivalence ratio was: $\theta' = (n' / \langle n' \rangle) \theta$.

D Droplet Size Measurement

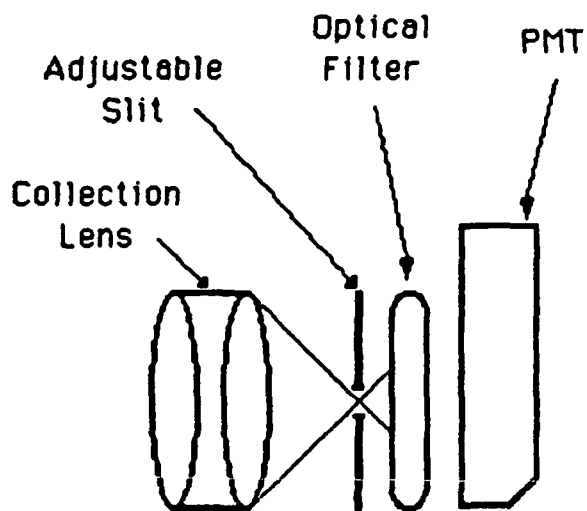
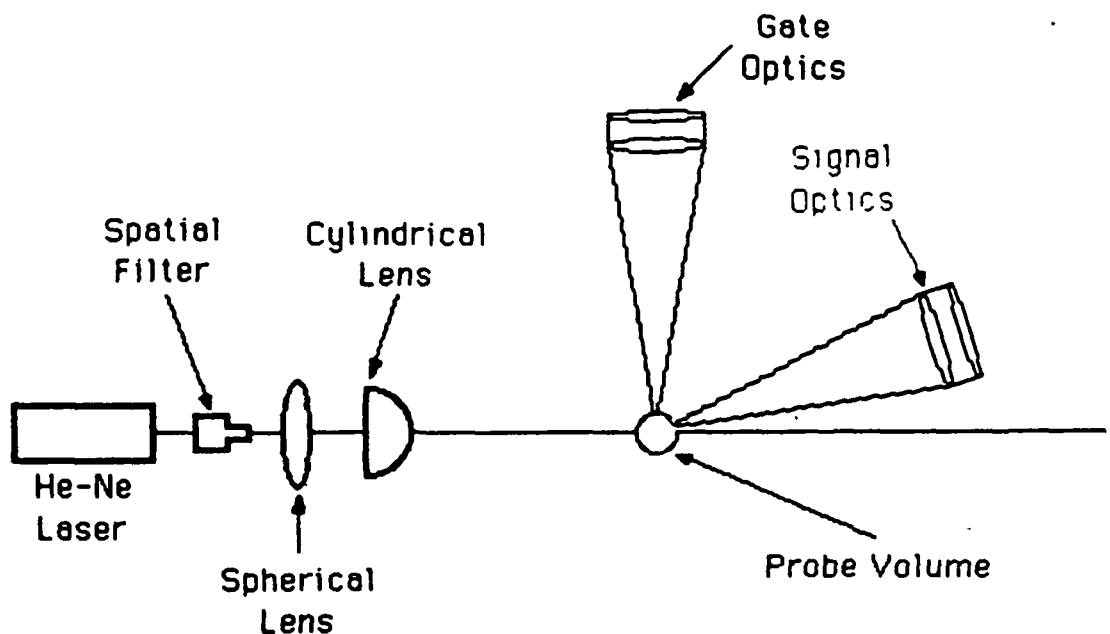
An apparatus has been designed which will provide the capability for measuring droplet size, and size distribution in the minimum ignition energy measurements. The technique is similar to those reported by Yule *et al.* (1977), Ungut *et al.* (1978), Holve and Self (1979), and Holve (1980) to obtain particle size distribution. Droplets which pass through a laser probe volume scatter light which is collected in the near forward direction. The measurement of the peak of the scattered signal is then related to the particle size. Due to the non-uniform illumination of the probe volume (Gaussian in the TEM_{∞} mode) and the characteristics of the collection optics, the scattered

light signal depends both on particle size and its trajectory through the probe volume. Holwe and Self (1979) have developed a deconvolution technique to unfold the particle size distribution from the distribution of measured peak signals from a large number of particles. In the present method a second gate detector is used to ensure that only particles passing through the center of the measurement volume are measured. The scattered light signal is then a unique function of particle size.

The method chosen is a non-intrusive technique capable of accurately measuring droplet size in the 10-100 μm range with a minimal dependence on the index of refraction. The computation of droplet size distribution becomes straight forward without the need for a deconvolution technique which invariably introduces error in the measurement of the particle size distribution. The system has good spatial resolution due to the small size of the measurement volume which is defined by the intersection of the two sets of collection optics. A detailed description of the hardware follows, and results of numerical computations to optimize the performance of the system will be presented in a later section.

The droplet size measuring system consists of a 35 mW He-Ne laser (632.8 nm wavelength), transmitting optics, and light collection optics which focuses the scattered light onto a photomultiplier tube. A second detector system is used to gate the signal from the primary detector. A schematic of the optical setup is shown in Figure 4. The transmission optics consist of a spatial filter and spherical lens which collimate the laser beam. An ellipsoidal probe volume is formed at the focus of the cylindrical lens when the collimated beam is passed through it. The dimensions of the probe length can be changed by using different focal length cylindrical and spherical lenses.

When the spray passes through the focused beam, it scatters the laser light. The near-forward scattered light is collected by the primary detector



Expanded View of Collection Optics

Figure 4. Optical Arrangement for Droplet Sizing

optics. This consists of a 55 mm f/1.4 camera lens, a pinhole for spatial filtering, and a 10 nm bandwidth laser interference filter. The scattered light is measured using a RCA 4840 photomultiplier tube. The gate detector system collects light scattered at 90°. For maximum flexibility, the gate detector system contains the same components as the primary detection system. Both detector systems are mounted on precision translation and rotation stages to allow extremely accurate positioning and alignment of the optical system

The signal processing system for the droplet sizing apparatus is shown in Figure 5. When a fuel droplet passes through the probe volume, defined by the intersection of the laser beam and the collecting optics field of view, nearly simultaneous Gaussian-type current pulses are produced by each of the photomultiplier tubes. Each of these pulses is processed on a single channel analyzer (SCA). When the signal peak occurs, each SCA sends a TTL-logic pulse to an adjustable one shot chip which then produces a variable-width TTL-logic pulse. The output from the two adjustable one shot chips are compared in an "and" gate. When these pulses overlap in time, the "and" gate outputs another TTL-logic pulse which triggers an analog-to-digital conversion of the primary signal detector output by the A/D converter of the LSI 11/2 based minicomputer. The data can then be stored on disk and later analyzed to obtain the droplet size distribution. A delay exists from the time the peak in the signal occurs until the signal is actually read by the A/D converter. This is due to the processing in the SCA and is of the order of one microsecond. Since the signal generated by the droplet has a width of about 100 microseconds (100 $\mu\text{m}/1 \text{ m/sec}$) there is only a slight error in measuring peak height with this apparatus. An estimate of the error in the peak height voltage, $V(0)$, can be

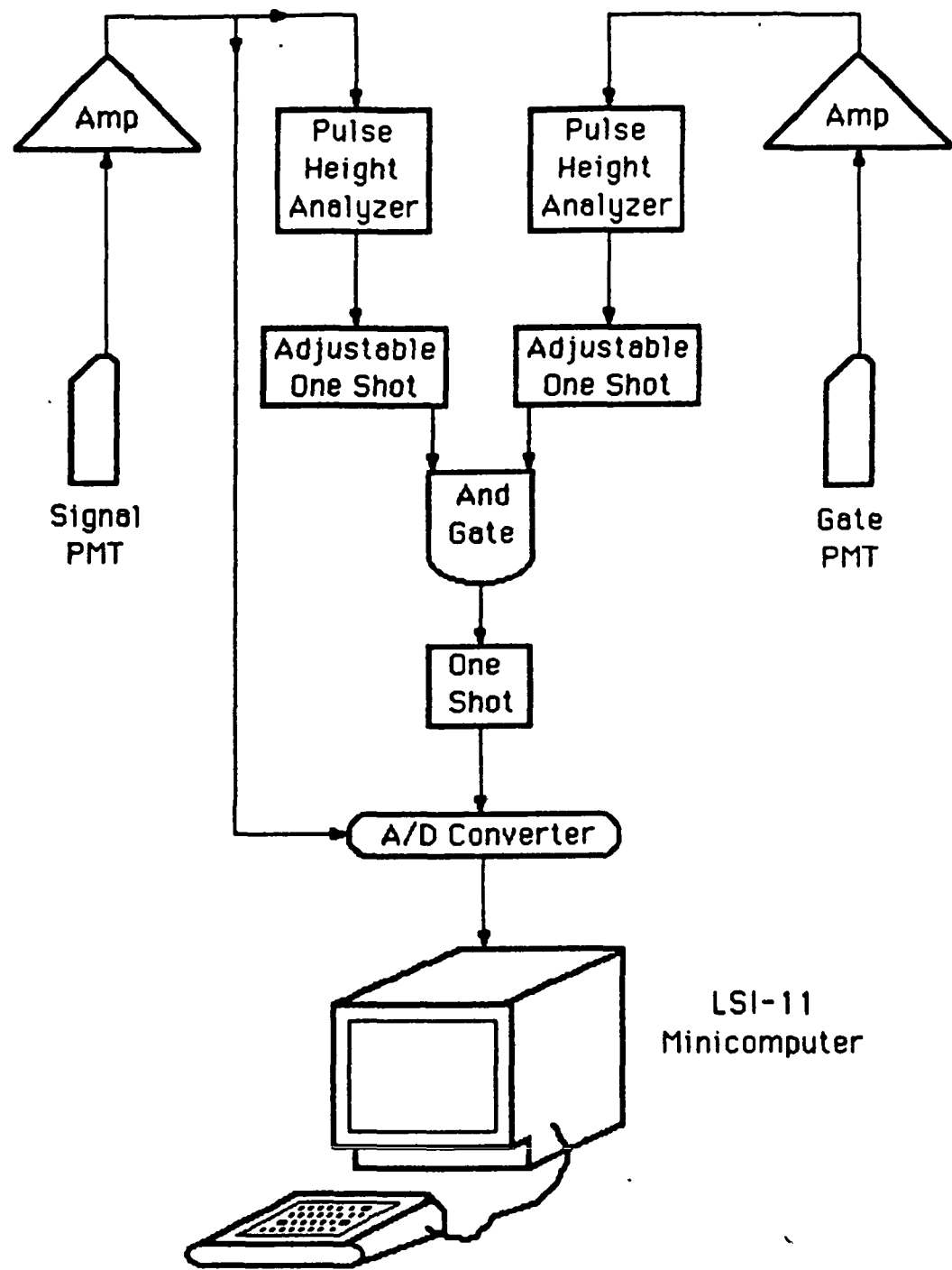


Figure 5. Schematic of Signal Processing System for Laser Droplet Sizing Apparatus

made by noting that the voltage $V(t)$ measured at a time t after the peak occurs is

$$V(\delta t) \approx V(0) + V''(0) \delta t^2 / 2$$

For a Gaussian signal

$$V = \exp[-t^2 / 2\sigma^2] / \sqrt{2\pi \sigma}$$

where σ is the standard deviation and

$$V''(0) = -V(0)/\sigma^2.$$

Therefore

$$\{V(0) - V(\delta t)\} / V(0) \approx 0.5 (\delta t / \sigma)^2.$$

If δt is 1 μ s and σ is about 25 μ s, the error in peak voltage measurement is 0.08% which is adequate for this experiment.

III. EXPERIMENTAL RESULTS AND DISCUSSION

A. Effect of Spark Duration on Minimum Ignition Energy

The effect of spark duration on ignition energy was tested initially with n-heptane sprays. Using a constant electrode spacing of 2.0 mm, ignition frequency measurements were made at two overall equivalence ratios (0.5 and 1.0) and two initial droplet diameters (28 and 68 μm) for each of five durations covering the range from 15 to 150 μs . For a given spark duration and spray condition, the ignition frequency was measured for 3-5 different spark energies ranging from 0.6 to 10 mJ. One hundred sparks were delivered to the spray at each spark energy, with the criterion for ignition being a visible flame. The spark energy was measured for 20 of the 100 sparks and the mean spark energy determined. The ignition frequency was then plotted against the mean spark energy. For each duration and spray condition, the spark energy which produced a 90% ignition frequency, as determined by a least mean squares straight line fit, was called the minimum ignition energy.

Figure 6 is a representative result of this duration study, showing the minimum ignition energy of a n-heptane spray of 68 μm initial droplet diameter and 1.0 overall equivalence ratio as determined by using five different durations ranging from 15-165 μs . As seen in Figure 6, spark duration had little effect on ignition energy, and this was the case for all conditions tested. Based on these results, spark durations in the 60-90 μs range were used for all subsequent ignition testing.

B. Spark Gap Equivalence Ratio Determination

The equivalence ratio at the spark gap, θ_G , was taken as the average of the local equivalence ratio, θ , over the width of the electrode spacing in the center of the spray. A representative graph of the variation in θ with radial position

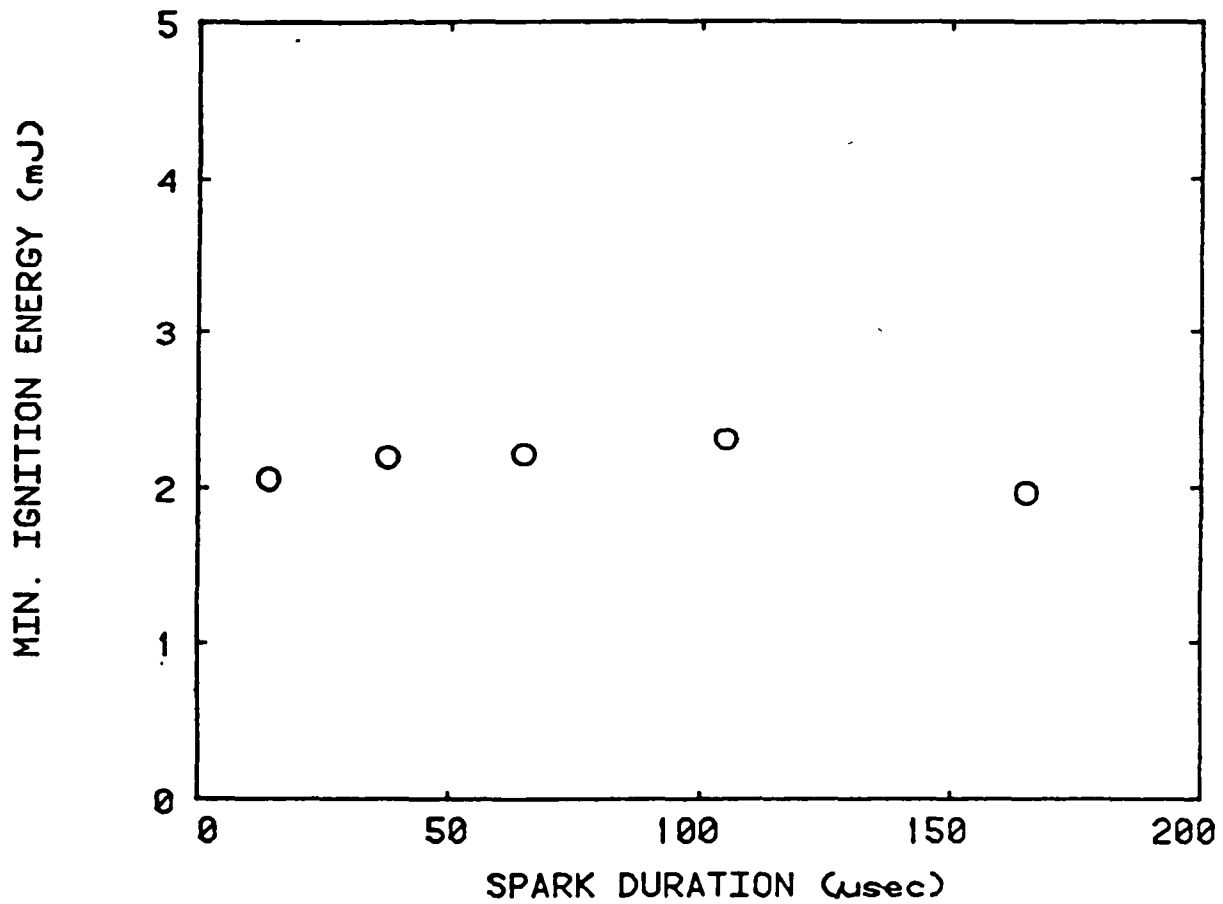


Figure 6. Effect of Spark Duration on the Minimum Ignition Energy of
N-Heptane Sprays: $D_0 = 68\mu\text{m}$, $\theta = 1.0$; Spark Gap = 20mm.

for three overall equivalence ratios for a spray of initial droplet diameter $D_0 = 50 \mu\text{m}$ is given in Figure 7. As seen in Figure 7, the local equivalence ratio had a parabolic profile across the test section, with the maximum droplet density at the center of the spray where the electrode spark gap was located. Therefore, θ_G was greater than θ in all cases. From data such as these, θ_G was determined for each spray condition studied.

C Optimization of Spark Gap Width

Previous spark ignition studies by other researchers (Rao and Lefebvre, 1973; Ballal and Lefebvre, 1978) have shown the electrode spacing to have an effect on the measured ignition energy of fuel sprays, with an optimum spark gap width observed. This optimum electrode spacing occurs due to the nature of spark ignition. The spark must raise the temperature of some volume of the fuel vapor/droplet and air mixture to its flame temperature in order to ignite it. This volume is called the spark kernel. In the case where the electrode spacing is smaller than optimum, more heat loss occurs from the spark kernel to the electrodes, and the kernel reaches a lower temperature. Conversely, when the spark gap width is larger than optimum, the volume of the spark kernel is larger and the kernel again reaches a lower temperature. Therefore, to accurately measure the minimum ignition energy of a spray, the optimum electrode spacing must first be determined.

For each spray condition studied, the spark gap width was optimized in the following manner. While keeping the spark energy constant, ignition frequency measurements were performed over a range of electrode spacings from 10 to 50 mm, in intervals of 0.5 mm. One hundred sparks were delivered to the spray at each spacing, and the spacing which produced the highest ignition

LOCAL EQUIVALENCE RATIO

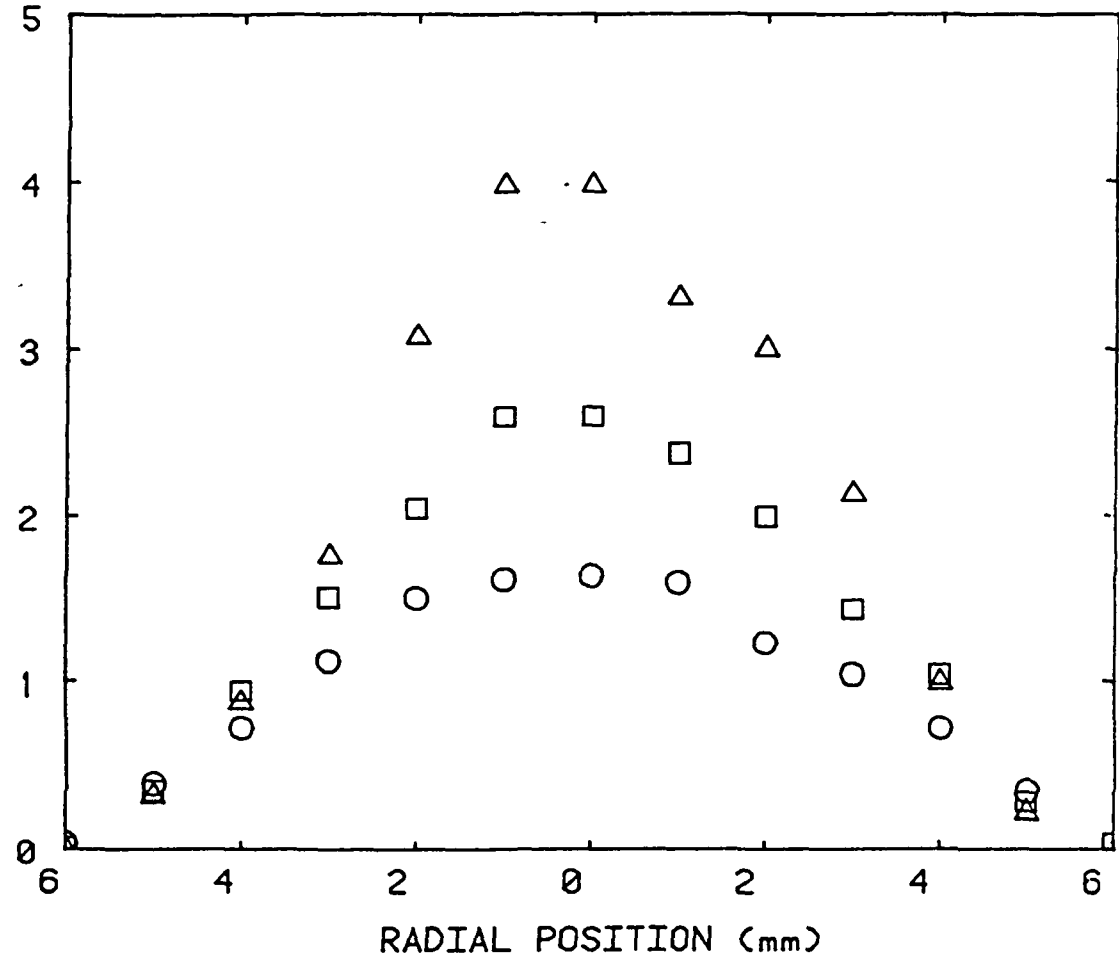


Figure 7. Radial Profiles of Local Equivalence Ratio (θ') Across the Test Section for N-Heptane Sprays

$D_0 = 50\mu\text{m}$, Spark Gap = 30mm, Spark Duration = 77 μs

($\Delta - \theta' = 1.0$, $\square - \theta' = 0.8$; $\circ - \theta' = 0.6$)

frequency was the optimum. Representative results from this optimization procedure are given in Figure 8, which shows the effect of spark gap width on ignition frequency for a spray of 70 μm initial droplet diameter and 1.0 overall equivalence ratio. As seen in Figure 8, 3.0 mm is clearly the optimum. In fact, 3.0 mm was the optimum spark gap width for all sprays studied with the exception of the 25 μm initial droplet diameter sprays, for which 3.5 mm was the optimum. All subsequent ignition energy testing was done using these optimum electrode spacings.

D. Droplet Size and Equivalence Ratio Effects on Minimum Ignition Energies

In order to determine the effect of droplet size and equivalence ratio on the minimum energy required to ignite n-heptane sprays, some criteria for that minimum had to be established. The ignition phenomenon is such that no sharp division exists between energies which are sufficient for ignition and those which are not. Instead, there is a range of energies for which ignition becomes more likely as the energy increases. Therefore, one can speak of a probability or frequency of ignition for a given spark energy. It was decided to denote the energy at which ignition was observed 90% of the time as the minimum ignition energy.

The minimum ignition energy was determined for a fuel spray of given initial droplet diameter and overall equivalence ratio in the following manner. Ignition frequency observations were made over a range of 3-5 different spark energies which produced ignition frequencies in the 70 to 100% range. At each spark energy, 150 to 250 sparks were used to determine the ignition frequency, and the actual spark energy of every fifth spark was measured to determine the mean spark energy. The ignition frequencies and their

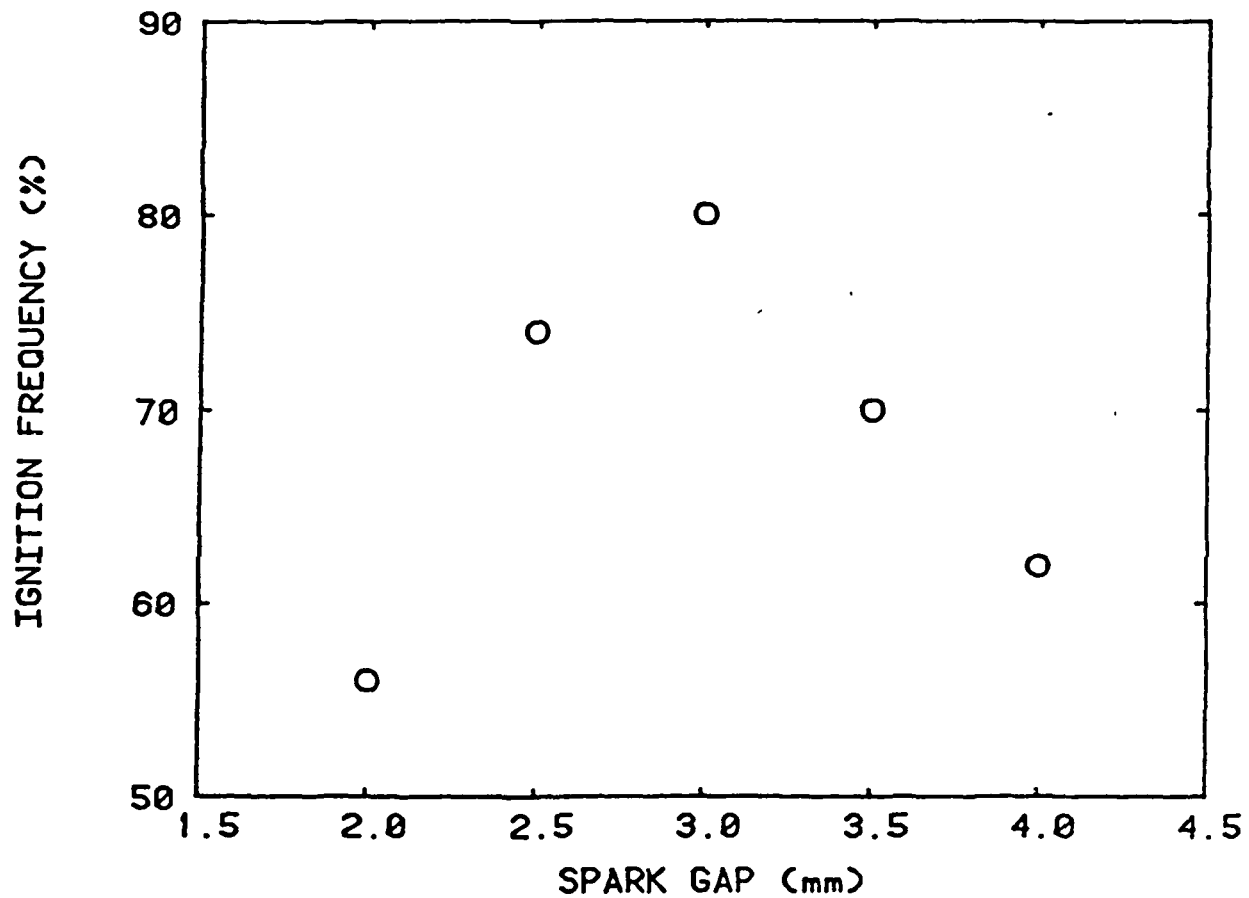


Figure 8. Effect of Spark Gap Width on the Frequency of Ignition for
N-Heptane Sprays:

$D_0 = 70\mu\text{m}$, $\theta = 1.0$, Spark Duration = $76\mu\text{s}$; Spark Energy = 0.8mJ

corresponding mean spark energies were then plotted. Representative data from this procedure are shown in Figure 9, which is for 60 μm initial droplet diameter sprays at gap equivalence ratios of 4.5, 3.5 and 2.5. The straight lines in Figure 9 were fit to the data by a least-squares method, and the minimum ignition energy (90% ignition frequency) was determined from these lines. This figure clearly shows that the ignitability of the sprays increased as the gap equivalence ratio increased.

From data such as that presented in Figure 9, the minimum ignition energy was determined for sprays with initial droplet diameters of 25, 40, 50, 60 and 70 μm , and gap equivalence ratios of 1.5, 2.5 and 3.5 (as well as two measurements at $\theta_G > 4.0$). Figure 10 shows the effect of varying droplet diameter on the minimum ignition energy for $\theta_G = 1.5, 2.5$ and 3.5. As seen in Figure 10, the minimum ignition energy of the sprays increased linearly as the initial droplet diameter increased from 25 to 70 μm at a given equivalence ratio. Also, the minimum ignition energy decreased as the gap equivalence ratio increased from 1.5 to 3.5 at a given droplet diameter. These results are in general agreement with the predictions based on an ignition model proposed by Ballal and Lefebvre (1981). The relevant part of their model applies to a heterogeneous, quiescent fuel/air mixture of monodisperse droplets. They further assumed that there was no prevaporation of droplets, while some prevaporation does occur in our experiments. Both the model and the data presented here predict a decrease in the minimum ignition energy with increasing equivalence ratio and decreasing initial droplet diameter. The main qualitative difference is that our experimental ignition energy data are represented better by a linear dependence on droplet diameter rather than the diameter cubed dependence predicted by the model. This may be due to the

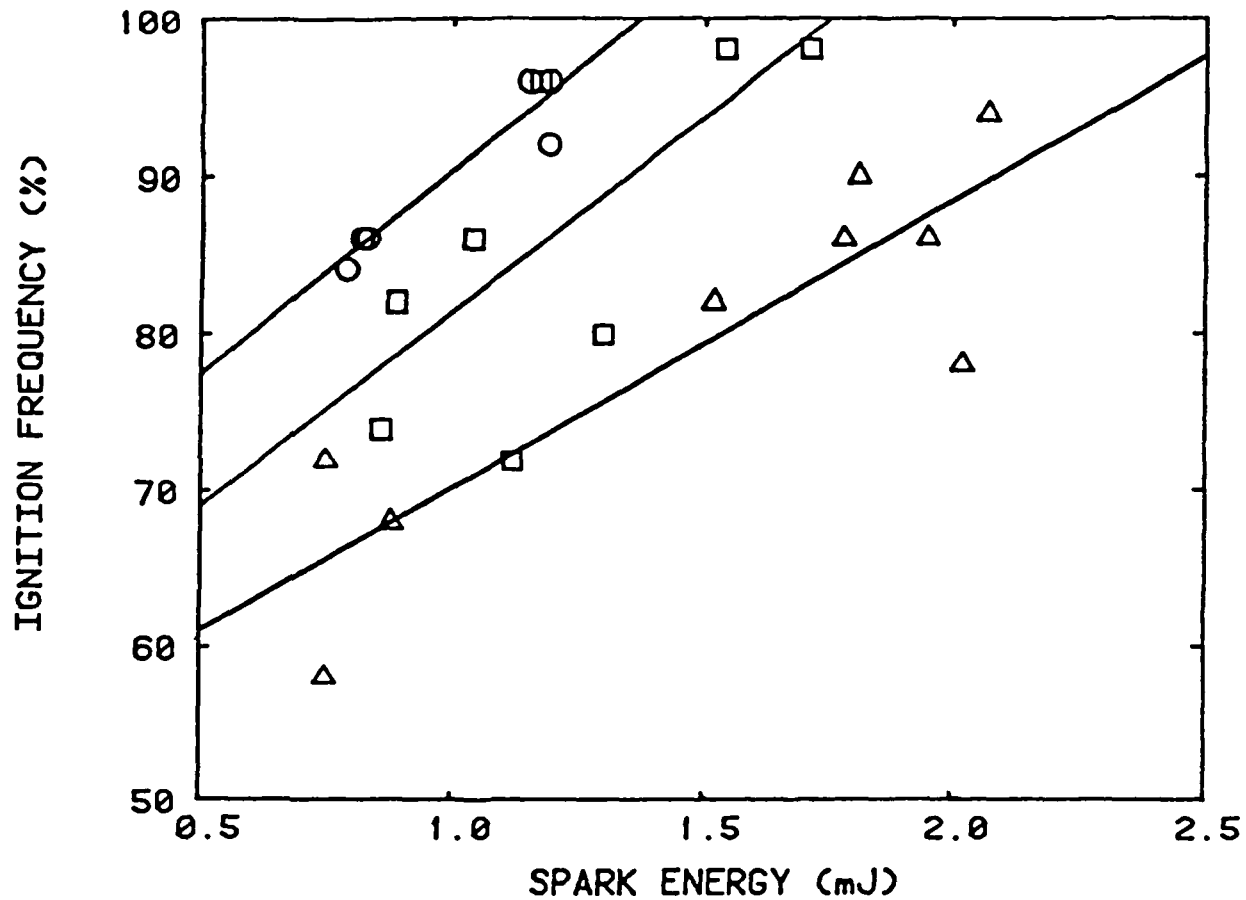


Figure 9. Effect of Gap Equivalence Ratio (θ_G) and Spark Energy
on the Frequency of Ignition for N-Heptane Sprays:

$D_0 = 60\mu\text{m}$; Spark Gap = 3.0mm; Spark Duration = 77 μs .

(○ - $\theta_G = 4.5$; □ - $\theta_G = 3.5$; Δ - $\theta_G = 2.5$)

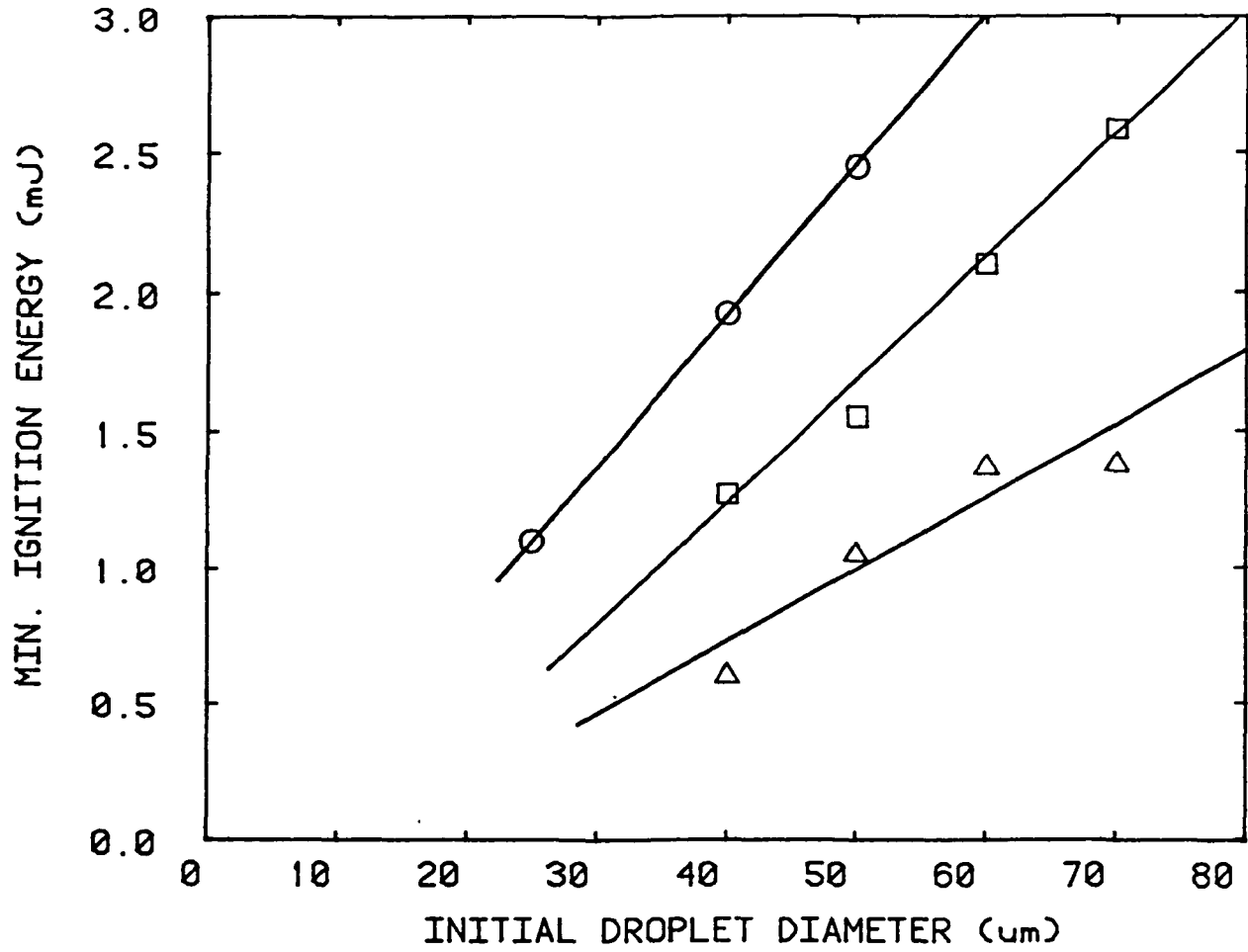


Figure 10 Effect of Gap Equivalence Ratio (θ_G) and Initial Droplet Diameter (D_0) on the Minimum Ignition Energy of N-Heptane Sprays.

(○ - $\theta_G = 1.5$, □ - $\theta_G = 2.5$; Δ - $\theta_G = 3.5$)

comparatively narrow range of droplet diameters studied here: 25-70 μm . Quantitatively, it was found that the ignition energies predicted by the model were always lower than the experimental values by 0.4-1.0 mJ.

A final observation concerning the results presented in Figure 10 is that the rate at which the minimum ignition energy increased with increasing droplet diameter decreased with increasing equivalence ratio. This would indicate that some optimum equivalence ratio, above $\theta_G = 3.5$, exists for ignition. This may seem to contradict the established convention that fuel/air mixtures ignite most readily at or near stoichiometric conditions. However, this stoichiometric condition only applies to prevaporized/premixed fuel/air mixtures, while most of the fuel within the spark gap is still in the liquid phase in our experiment. Therefore the average equivalence ratio in the gas phase region between the droplets in the spark gap will be considerably lower than θ_G , which includes the liquid phase fuel as well. For this reason, one must expect phenomena which are usually associated with stoichiometric conditions to occur at considerably richer values of θ_G . This is essentially the same conclusion which was reached by Aggarwal and Sirignano (1984).

An optimum droplet size for ignition was not observed in this study. If such an optimum exists, it would be below 25 μm initial droplet diameter for the conditions examined in this work. This has also been suggested by work done by Chan and Polymeropoulos (1981).

E Droplet Sizing Method

The most important theoretical aspect of the droplet sizing system is the sensitivity of the measurement system to droplet size. The sensitivity of the system to droplet size is a function of the collection geometry, and the optical properties of the droplet. A computer code was developed which simulates the response of the system as a function of droplet size, collection geometry, and droplet optical properties. A brief discussion of the theory behind the code is presented, followed by the results of the computations.

The scattered light intensity from a spherical particle can be written as

$$I = [I_0 / (k^2 r^2)] \cdot F(\alpha, \phi; n) \quad (\text{van de Hulst, 1957})$$

where: I_0 - Incident intensity on the particle.

k - Wave number of the incident radiation.

α - Scattering parameter ($\alpha = \pi D/\lambda$)

D - Particle diameter

λ - Wavelength of the incident radiation.

n - Complex index of refraction

F - Scattering function

ϕ - Scattering angle relative to optical axis

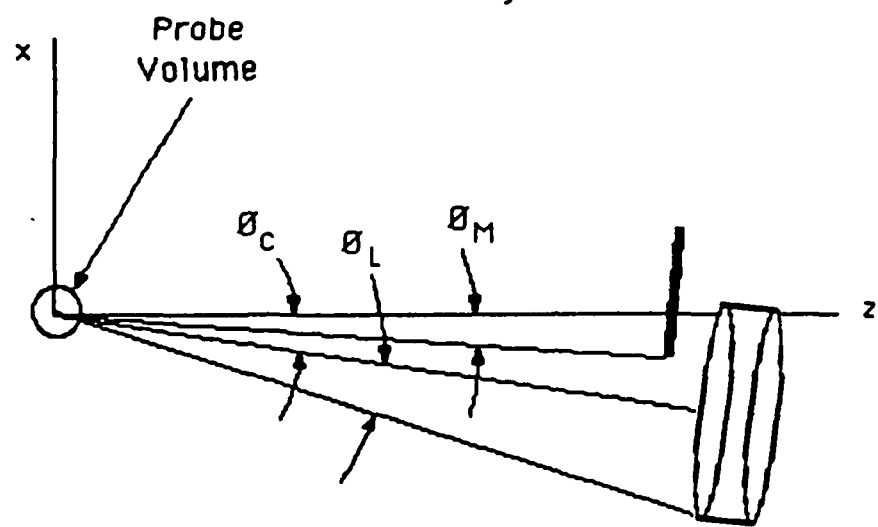
The response function is defined as the scattered light intensity integrated over the surface of the collection optics, and is proportional to the output of the photomultiplier tube. Using the equation for the scattered intensity above, the response function is written as

$$RF = [I_0 / k^2] \cdot \int_S F(\alpha, \phi, n) d\sigma$$

The scattering function, F' , has been computed from Mie scattering theory, using subroutines from Wiscombe (1979). Results have also been computed using Fraunhofer diffraction theory to determine the scattering function. Hodgkinson and Greenleaves (1963) found that in the limit of large particles, Mie theory can be approximated by the separate effects of diffraction, reflection, and refraction. If a significant portion of the signal is due to diffraction, the dependence on the index of refraction and polarization of the incident radiation will be minimized. This is the reason a near forward geometry is used. Holwe (1979) investigated a coaxial geometry, but found that the measurement volume was too large, and errors due to two particles in the probe volume simultaneously became significant. If part of the lens is masked off, then it is possible to collect more light at smaller angles, thus capturing more of the diffracted component. This geometry is shown in Figure 11, along with all other angles used in the calculations. Computations of the response function have been made for a wide range of collection geometries and refractive indices. The test conditions are presented in Table 1. Results representative of the computation for Mie theory are shown in Figs. 12 and 13.

Both of these and all subsequent plots have the computed response function as a function of the scattering parameter for fixed collection geometry and droplet refractive index. It should be noted that for He - Ne laser light the droplet diameter $D = \alpha / 10$. Figure 12 shows that the response function is a monotonically increasing function of the scattering parameter. This is the desired result since the output of the PMT would uniquely define particle size. A different collection geometry and refractive index result in the plot of Figure 13. In this case, the response function will no longer uniquely define particle size. The reason these computations are performed is to optimize the design of the system and eliminate or minimize the sizing ambiguity of Fig. 13.

Projection in the x-z plane.



Projection in the x-y plane.

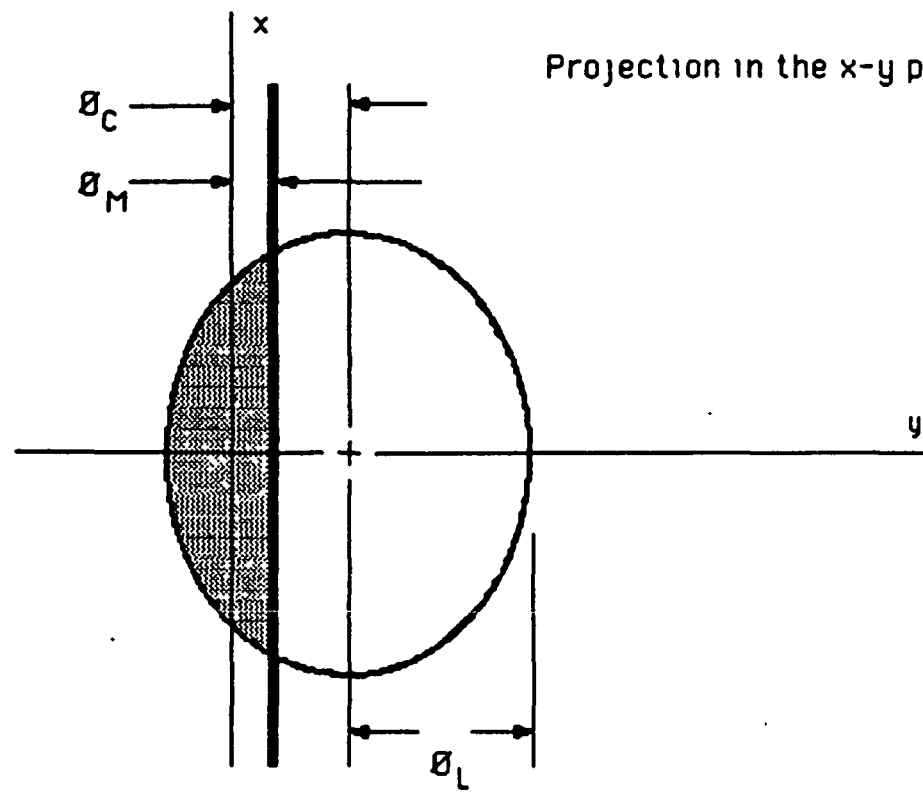


Figure 11. Collection Geometry

Table 1. Computational Matrix

Test	Collection Angle	Collection Aperture	n_1	n_2	Mask Angle
1. n_2 Variation Tests	Fixed	Fixed	Fixed	0.0,0.001, 0.01,0.1	Fixed
2. n_1 Variation Tests	Fixed	Fixed	1.2,1.4, 1.6,1.8	Vary over above range	Fixed
3. Collection Aperture Variation	Fixed	5°,10°,12.3° 16.3°,20°,25°	Vary over above range	Vary over above range	Fixed
4. Collection Angle Variation	1°,2°,4° 6°,8°,10°	Vary over above range	Vary over above range	Vary over above range	Fixed
5. Mask Angle	Vary	Vary	Vary	Vary	5 mask angles to be chosen

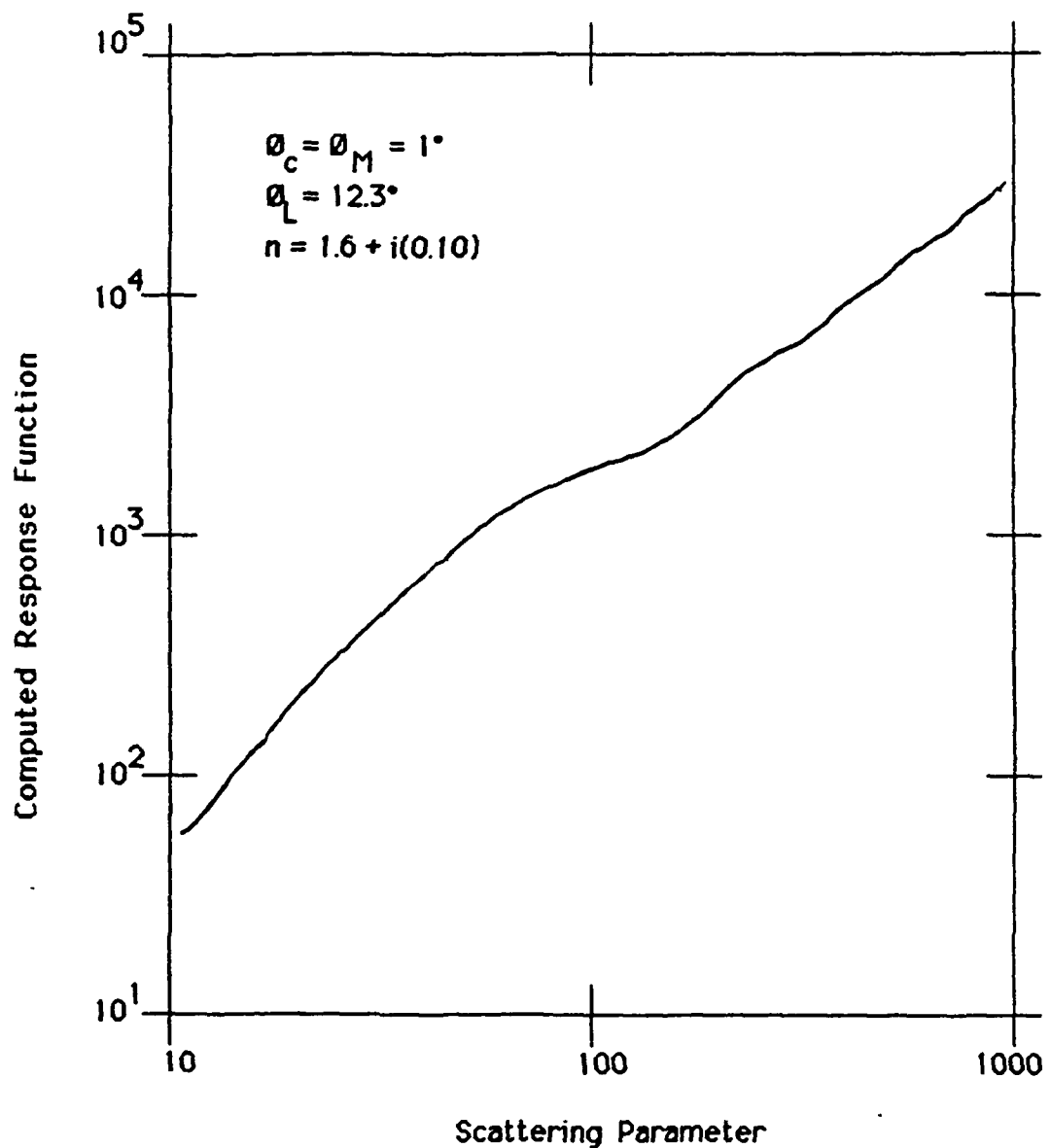


Figure 12. Computed Response Function using Mie Theory, Optimized System

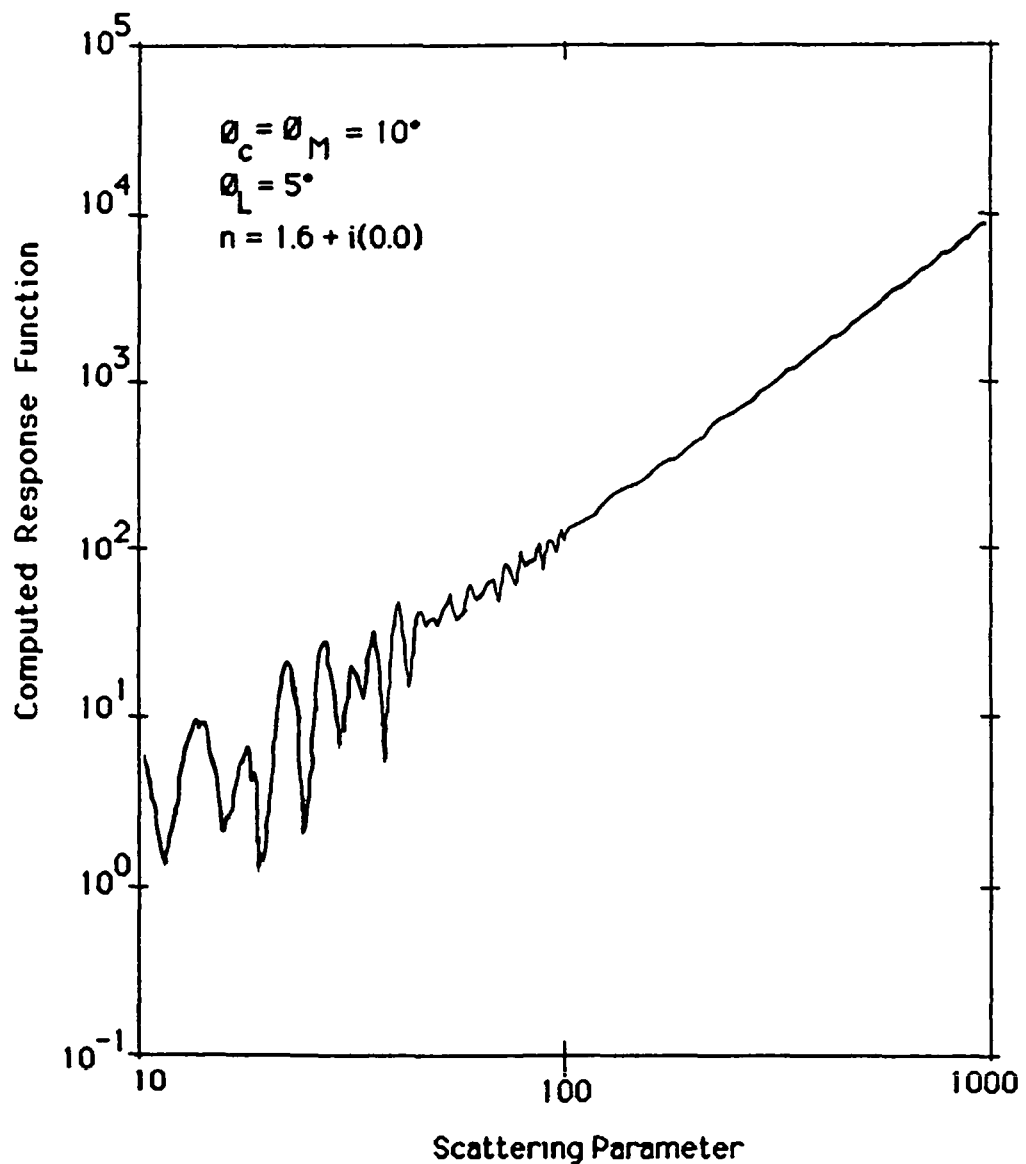


Figure 13. Computed Response Function using Mie Theory,
Non - Optimized System

This optimization is based on the minimization of the parameter R defined as

$$R = 2 ((\alpha_L - \alpha_S) / (\alpha_L + \alpha_S))$$

where α_L and α_S are the large and small values of the scattering parameter for which a sizing ambiguity exists. The location of the maximum value of R is also important. For this work the maximum value of R was always found to be in the $\alpha \approx 10$ to $\alpha = 100$ range ($D = 1$ to $10 \mu\text{m}$). The computations have been performed to determine the effects of collection geometry and droplet refractive index on the parameter R.

The effect of increasing the collection aperture (θ_L) is shown in Figure 14. The response function has been shown as a function of scattering parameter for different collection apertures and fixed collection angle and droplet refractive index. For a collection aperture of 5° , the maximum value of R is 0.51. The maximum value of R decreases to 0.40 as the collection aperture is increased to 20° . The effect of increasing the collection angle is therefore to improve the resolution of the system. Similar collection aperture behavior is observed regardless of the value of the collection angle or refractive index. Only the magnitude and location of the maximum R will change. However, the effect becomes more pronounced as the collection angle is increased.

Figure 15 shows the effect of increasing the collection angle (θ_C) on the computed response function (fixed collection aperture and refractive index). For a collection angle of 10° , R is 0.96, and as the collection angle is decreased to 1° , the maximum value of R is decreased to 0.45. The resolution of the system will improve as the collection angle is decreased.

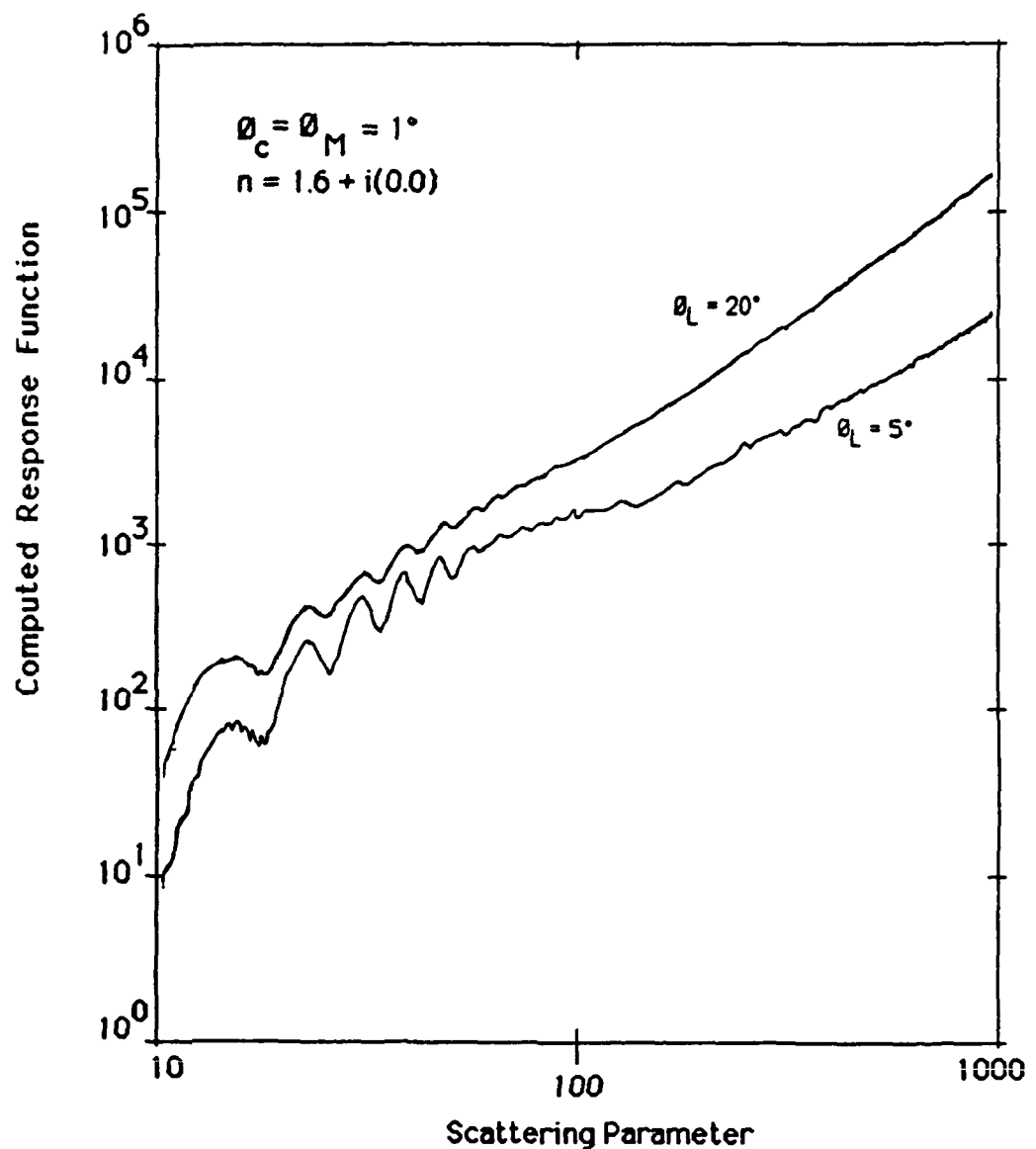


Figure 14 The Effect of Collection Aperture (ϕ_L) on
the Computed Response Function

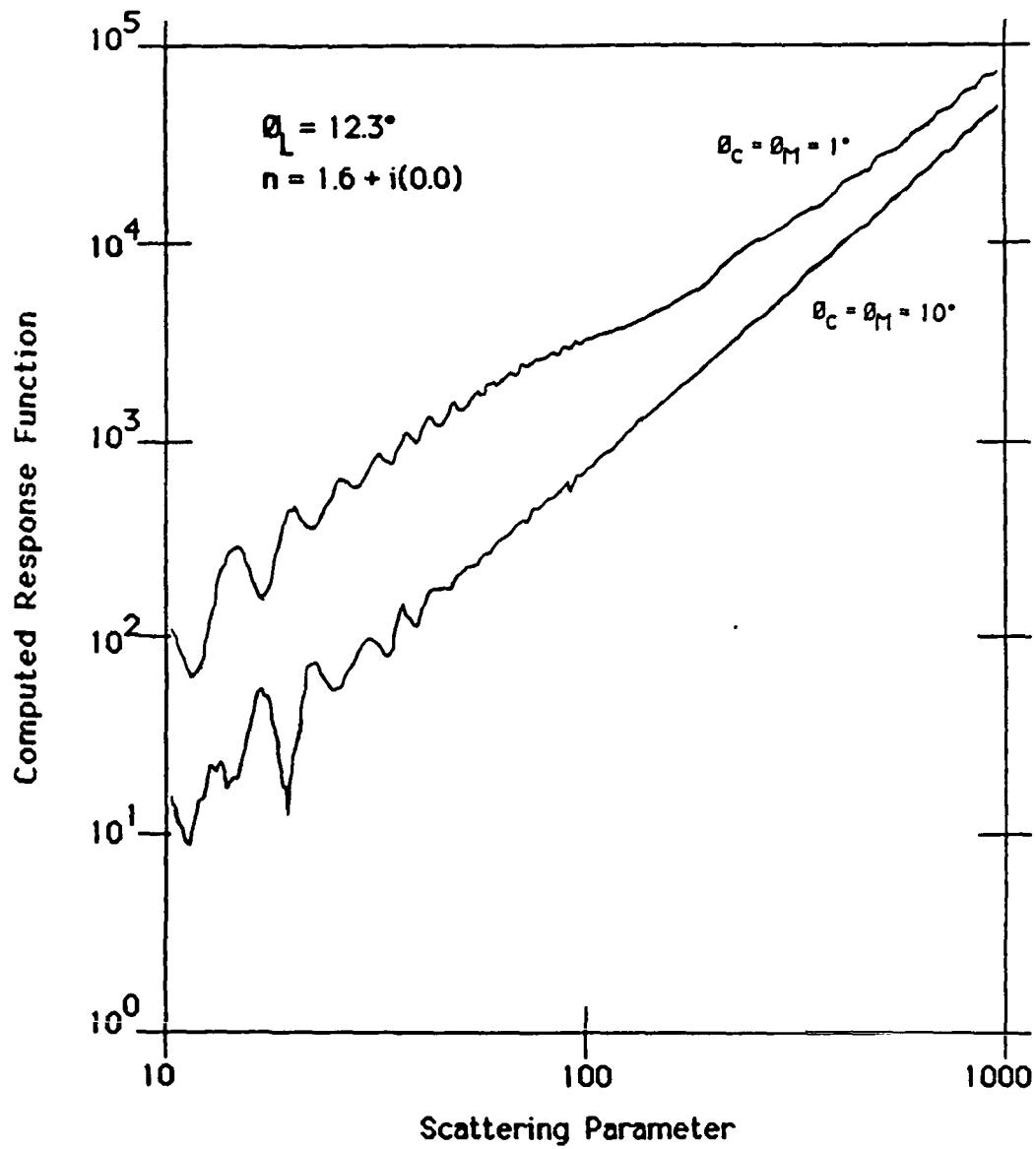


Figure 15 The Effect of Collection Angle (ϕ_C) on
the Computed Response Function

This trend is independent of collection aperture and refractive index although the magnitude and location of the maximum R does change.

The optimum geometry will then have as small a collection angle and as large a collection aperture as possible. Signal coincidence effects in the probe volume may require the use of larger collection angles to reduce the size of the probe volume. If this is the case, a larger collection aperture can be used to partially offset the reduction of sensitivity due to a larger collection angle. The results have shown that the effect of decreasing the collection angle was stronger than that of increasing the collection aperture.

The effect of the imaginary part of the complex index of refraction on the response function is shown in Figure 16. This figure clearly shows that when the imaginary part of the index of refraction of a particle is increased from 0.0 to 0.1, the resolution of the system is improved. For an imaginary part of the index of refraction of 0.1 the response function becomes a monotonically increasing function of the scattering parameter for the collection geometries shown. The calculations have shown that this trend is independent of the collection geometry and real part of the refractive index. Results have been tabulated for variations of the real part of the refractive index. Although the shape of the response function curve does change, the resolution, as measured by R, is not affected by variations in the real part of the refractive index.

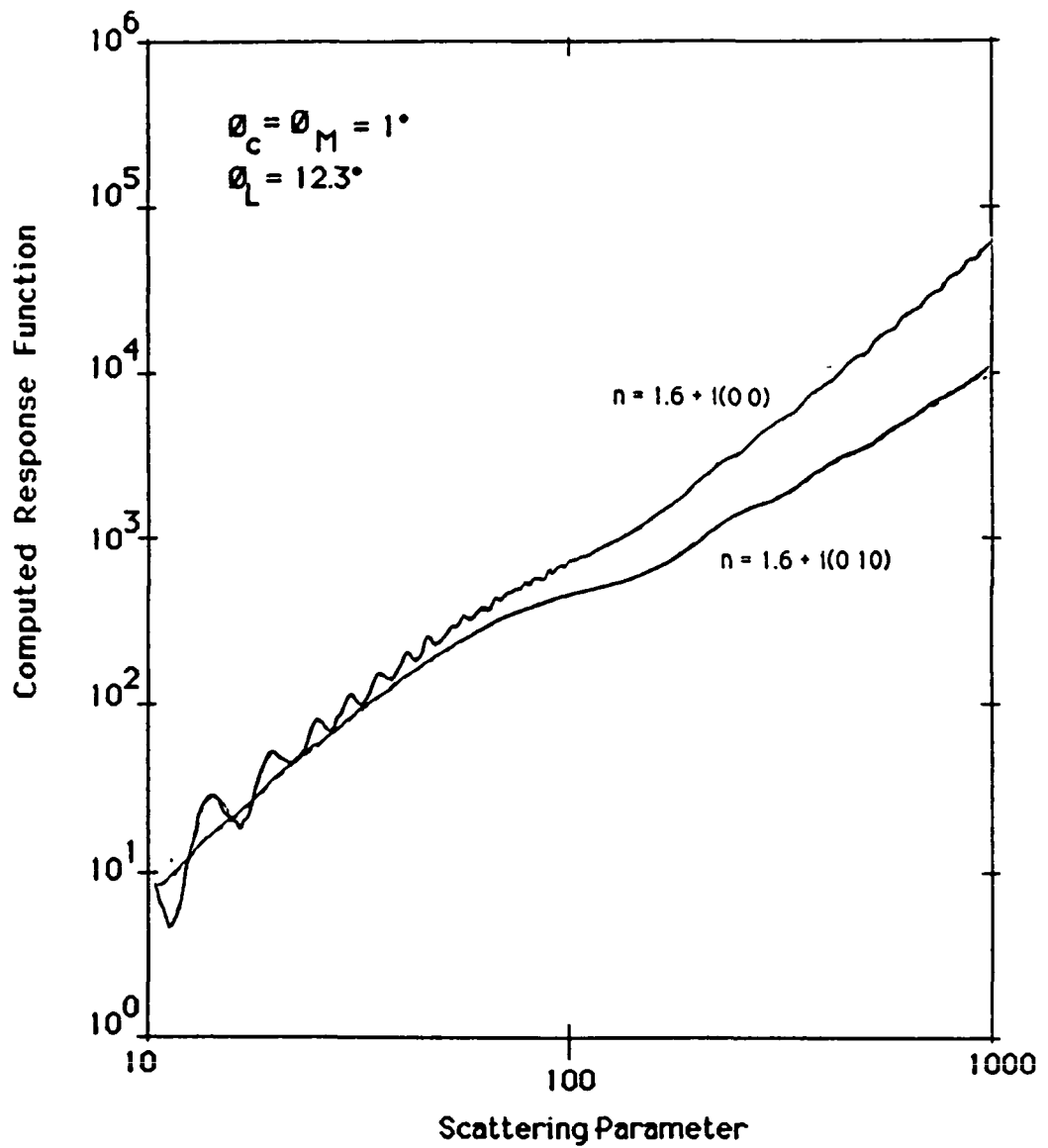


Figure 16. The Effect of the Imaginary Part of the Index of Refraction on the Computed Response Function

F. Summary and Conclusions

A reliable facility for studying the details of spray combustion for liquid droplets in the transition region ($10\text{-}100 \mu\text{m}$ initial diameter) has been developed and minimum spark ignition energies for n-heptane have been measured. The following conclusions regarding the present ignition studies can be drawn:

- (1) For initial droplet diameters of 28 and $68 \mu\text{m}$ and overall equivalence ratios of 0.5 and 1.0 , spark duration had little effect on minimum ignition energy.
- (2) In all cases where local droplet number density was measured, the spark gap equivalence ratio was found to be greater than the overall equivalence ratio.
- (3) For all but the smallest initial droplet size studied ($25 \mu\text{m}$), the optimum spark gap width was determined to be 3.0 mm . This value increased slightly to 3.5 mm for $25 \mu\text{m}$ diameter droplets.
- (4) For a range of initial droplet diameters of $25\text{-}70 \mu\text{m}$ and gap equivalence ratios from 1.5 to 3.5 , the minimum ignition energy of the sprays increased linearly with initial droplet diameter and decreased as the gap equivalence ratio was increased. These results followed the trends predicted by Ballal and Lefebvre (1981); however the dependence of minimum ignition energy on initial diameter was not as strong as their model predicts (linear dependence observed rather than the d^3 dependency predicted).
- (5) Ignition energies measured in the present work always exceeded the predicted values of Ballal and Lefebvre by $0.4\text{-}1.0 \text{ mJ}$.

- (6) The rate of increase of minimum ignition energy with droplet diameter was reduced as spark gap equivalence ratio was increased, indicating that some optimum equivalence ratio greater than $\Phi_G = 3.5$ (highest value studied) exists. This is essentially the conclusion drawn for heterogeneous systems by Aggarwal and Sirignano (1984)

Further work on minimum ignition energy is planned for more complicated spray systems including binary mixtures. Also, smaller initial droplet sizes will be studied ($< 25 \mu\text{m}$) to determine the dependence of minimum ignition energy at the lower end of the transition region. Eventually, more precise measurements of spark gap equivalence ratio and droplet size at the gap will be provided by the optical droplet sizing technique. These data will provide the true droplet size effect on minimum ignition energy as well as a better knowledge of droplet evaporation rates.

The laser-based forward scattering droplet sizing technique has not yet been implemented to make actual droplet size measurements on the spray burner. This is due to delays in the development of the complex computer code which makes the response function calculations. In addition, it was decided to carry out a series of numerical studies with the code in order to obtain desirable information for setting up the optics for actual droplet size measurements. Conclusions which can be drawn from these studies are:

- (1) The optimum collection geometry for maximizing the resolution of the droplet sizing system (minimizing R) should have the smallest possible collection angle with the largest possible collection aperture
- (2) Increasing the imaginary part of the refractive index (absorption) tends to smooth the resonant structure of the response function curve, and increase the resolution of the system.

(3) The resolution of the droplet sizing system will be a very weak function of the real part of the refractive index.

In addition to the numerical studies presented, the transmitting optics and one set of collection optics have been set up and aligned. Work in the immediate future will center on the implementation of the electronic signal processing equipment to the existing optical set up. Upon completion of this task, a system calibration will be performed after which the system will be used to measure droplet size, droplet size distribution, and number density in the spray experiments.

Additional work will also be performed on the computer code to include probe volume and collection optics effects on the computed response function. The code will also be used to examine the possibility of modifying the present system to measure droplet size and size distribution using an intensity ratioing technique.

IV REFERENCES

- Aggarwal, S. K. and Sirignano, W. A.,
"Ignition of Fuel Sprays: Deterministic Calculations for Idealized Droplet Arrays," Twentieth Symposium (International) on Combustion, p. 1773-1780, The Combustion Institute, Pittsburgh, PA, 1984.
- Ballal, D. R. and Lefebvre, A. H.,
"Ignition and Flame Quenching of Quiescent Fuel Mists," Proc. R. Soc. Lond., A364, pp. 277-294, 1978.
- Ballal, D. R. and Lefebvre, A. H.,
"A General Model of Spark Ignition for Gaseous and Liquid Fuel-Air Mixtures," Eighteenth Symposium (International) on Combustion, p 1737-1745, The Combustion Institute, Pittsburgh, PA, 1981.
- Berglund, R. N. and Liu, B. Y. H.,
"Generation of Monodisperse Aerosol Standards," Environmental Science and Technology 7, 2, 147, 1973
- Chan, K. K. and Polymeropoulos, C. E.,
"An Experimental Investigation of the Minimum Ignition Energy of Monodisperse Sprays," Paper No. ESSCI 81-21, Fall Technical Meeting, Eastern States Section, The Combustion Institute, Pittsburgh, PA, October 1981.
- Danis, A. M., Cernansky, N. P. and Namer, I.,
"Transition Region Ignition Characteristics of N-Heptane Fuel Sprays," Paper No. CSS/WSSCI 85-1-6B, Joint Western and Central States Section, The Combustion Institute, San Antonio, TX, 22-23 April 1985.
- Hodkinson, J. R. and Greenleaves, I.,
"Computations of Light-Scattering and Extinction by Spheres According to Diffraction and Geometrical Optics, and Some Comparisons with Mie Theory," J. Opt. Soc. Am. 53, 5, 577-588, 1963
- Holve, D. and Self, S.,
"Optical Particle Sizing for In-Situ Measurements, Parts I and II," J. Appl. Optics 18, 10, 1979.

Holve, D.,
"In-Situ Particle Sizing Technique," J Energy 4, 176, 1980

Rao, H. N. S. and Lefebvre, A. H.,
"Ignition of Kerosine Fuel Sprays in a Flowing Air Stream,"
Combustion Science and Technology 8, 95, 1973

Ungut, A , Yule, A. J , Taylor, D C. and Chigier, N. A ,
"Particle Size Measurement by Laser Anemometry," J Energy 2, 6,
1978.

van de Hulst, H. C ,
Light Scattering by Small Particles, Dover Publications, New York, New
York, 1957

Wiscombe, W J.,
"Mie Scattering Calculations. Advances in Technique and Fast, Vector
Speed Computer Codes," Report No. NCAR/TN - 140 + STR, National
Center for Atmospheric Research, Boulder, Colorado, June 1979

Yule, A. J., Chigier, N A , Atakan, S. and Ungut, A.,
"Particle Size and Velocity Measurement by Laser Anomometry," J
Energy 1, 4, 1977.

APPENDIX: PUBLICATIONS AND PRESENTATIONS

In addition to the semi-annual progress reports and this final report, work accomplished as part of this and related research programs has resulted in the following publications and presentations:

- (1) Nizami, A. A and N P Cernansky, "A Monodisperse Spray Combustion System and the Measurement of Oxides of Nitrogen," Paper No. WSSCI 78-37, presented at the 1978 Western States Section/Combustion Institute Spring Meeting, Boulder, CO, 17-18 April 1978
- (2) Nizami, A. A., "An Experimental Study of NO_x Formation in Monodisperse Fuel Spray Combustion," Ph.D. Thesis, Drexel University, Philadelphia, PA, 1978.
- (3) Nizami, A. A and N P. Cernansky, "NO_x Formation in Monodisperse Fuel Spray Combustion," Seventeenth Symposium (International) Combustion, The Combustion Institute, Pittsburgh, PA, p. 475-483, 1979
- (4) Nizami, A. A. and N. P. Cernansky, "Some Aspects of Pollutant Formation in Spray Combustion of Certain Hydrocarbon Fuels," presented and published in the Sixth National Conference on Combustion and Internal Combustion Engines, IIT Bombay, December 1979
- (5) Nizami, A. A., S. Singh and N P Cernansky, "Formation of Oxides of Nitrogen in Monodisperse Spray Combustion of Hydrocarbon Fuels," Combustion Science and Technology 28, 97-106, 1982.
- (6) Nizami, A. A., R A. Recchiuti and N P. Cernansky, "Chemiluminescent Measurements of Oxides of Nitrogen from Combustion Systems," Department of Mechanical Engineering and Mechanics Report, Drexel University, Philadelphia, PA, May 1982.
- (7) Sarv, H., A. A. Nizami and N. P. Cernansky, "Droplet Size Effects on NO_x Formation in a One-Dimensional Monodisperse Spray Combustion System," ASME Paper No. 82-JPGC-GT-10, presented at the 1982 Joint Power Generation Conference, Denver, CO, 17-21 October 1982.

- (8) Cernansky, N. P. and H. Sarv, "Air Preheating and Droplet Size Effects on NO_x Formation in a One-Dimensional Monodisperse Spray Combustion System," Ninth International Colloquium on Dynamics of Explosions and Reactive Systems, Poitiers, France, 4-8 July 1983.
- (9) Sarv, H., "Droplet Size Effects on NO_x Formation in a One-Dimensional Monodisperse Spray Combustion System," PhD Thesis, Department of Mechanical Engineering and Mechanics, Drexel University, Philadelphia, PA, June 1985.
- (10) Danis, A. M., N. P. Cernansky and I. Namer, "Transition Region Characteristics of N-Heptane Fuel Sprays," Paper No. CSS/WSSCI 85-1-6B, presented at the 1985 Spring Technical Meeting of the Central and Western States Sections/Combustion Institute, San Antonio, TX, 22-23 April 1985
- (11) Dietrich, D. L., N. P. Cernansky and I. Namer, "Optimization of a Droplet Sizing Apparatus for in situ Measurements," Paper No ESSCI 85-79, presented at the 1985 Eastern States Section/Combustion Institute Technical Meeting, Philadelphia, PA, 4-6 November 1985
- (12) Danis, A. M., I. Namer and N. P. Cernansky, "Minimum Ignition Energies of Rich N-Heptane Fuel Sprays in the Transition Region," Paper No ESSCI 85-26, presented at the 1985 Eastern States Section/Combustion Institute Technical Meeting, Philadelphia, PA, 4-6 November 1985
- (13) Sarv, H. and N. P. Cernansky, "Analysis of the Effects of Fuel Spray Characteristics on NO_x Formation," Paper No. ASME 85-WA/HT-47, presented at the ASME Winter Annual Meeting, Miami Beach, FL, 17-22 November 1985.
- (14) Danis, A. M., N. P. Cernansky and I. Namer, "Ignition Characteristics of N-Heptane Fuel Sprays in the Transition Region," Paper No ASME 85-WA/HT-46, presented at the ASME Winter Annual Meeting, Miami Beach, FL, 17-22 November 1985.

Copies of these papers or reports can be obtained by writing

Dr Nicholas P Cernansky
Department of Mechanical Engineering and Mechanics
Drexel University
Philadelphia, PA 19104 (215) 895-2284, 2352